

# Response to reviewers: “A new Digital Elevation Model of Antarctica derived from CryoSat-2 altimetry”

Thomas Slater, Andrew Shepherd, Malcolm McMillan, Alan Muir, Lin Gilbert, Anna E. Hogg, Hannes Konrad, Tommaso Parrinello

We would like to thank each of the three reviewers for their positive and constructive reviews of our manuscript. In our response to each individual comment we outline where we have made changes according to suggestions which we agree improve the manuscript, or provide detailed reasoning where we have chosen to not make changes.

## Summary of changes to manuscript:

1. Figures 1 and 8 have been changed to bar plots for readability.
2. Latitude and longitude grids have been added to Figures 2,3,4,5,6 and 7.
3. The colour scales of Figures 6 and 7 have been changed for readability.
4. A new supplementary material document has been created with information about our data filtering approach, and an uncertainty map for the DEM.
5. Several minor changes to the text with improvements suggested in the referee comments.

## Response to specific comments

Please find below response to each of the reviewers comments in turn. Reviewer comments are in *black italic*, our responses are in [blue](#).

### Anonymous Referee #1

**1.** *Page 1 Line 24: “surface elevation is essential for delineation of drainage basins” – this is not totally true – although early work on drainage basins (early Rignot and Zwally papers), used surface slope to delineate drainage, later Rignot papers used flow and flow direction which is a more robust method. I would temper the sentence by saying “can be used” rather than are essential.*

[Agreed, we have amended the sentence to reflect this:](#)

“Accurate knowledge of surface elevation can be used for both the delineation of drainage basins and estimation of grounding line ice thickness, necessary for estimates of Antarctic mass balance calculated via the mass budget method (Rignot et al., 2011b; Shepherd et al., 2012; Sutterly et al., 2014).”

**2.** *Page 2 line 5: It might be worth adding that over rock outcrops and steeper slopes, where cryostat coverage is poorer, the photogrammetric models do perform better and so act as an alternative in these regions.*

Agreed, we have amended the sentence to reflect the performance of this technique over bare rock and steep slopes.

“Although these photogrammetric models perform well over regions of bare rock and steep slope found in the margins, their accuracy is considerably reduced in ice covered areas.”

**3.** *Page 3 line 30. Reading the text I was a little unsure if the figures (percentages) included the polar hole or not. Please clarify.*

All stated percentages include the pole hole – after integrating the re-sampled 2 km and 5 km DEMs we have a data coverage of 94%, and we then interpolate any unobserved grid cells outside the pole hole, which accounts for 5% of the ice sheet area. This leaves 1%, which represents the area of the pole hole. We have amended this sentence to make this clearer.

“At a resolution of 1 km, the model fit provides an elevation estimate in 60 % and 75% of grid cells within the total area of the ice sheet and ice shelves, respectively.”

**4.** *Page 4 line 10: Why use Kriging? There are lots of alternative interpolation methods, all will give slightly different results, but you do not say why this method was chosen rather than the others. Do you have any evidence that this is the best method to use?*

Our use of Kriging is in line with the generation of previous DEMs derived from satellite altimetry within the literature (Bamber et al., 2009; Helm et al., 2014). Ordinary kriging is a geostatistical approach which takes into account the distribution of values around the location to be interpolated, and as such is an appropriate technique for interpolating elevation. We have amended and added citations to this sentence to make this clearer:

“In order to provide a continuous dataset, we estimate elevation values in grid cells North of 88 ° S that contain no data using ordinary kriging (Isaaks and Srivastava, 1989; Kitanitis 1997), an interpolation technique used in the generation of previously published DEMs (Bamber et al., 2009; Helm et al., 2014).”

5. A slight grammatical point on page 7 and through the text; the phrase “At the Antarctic Peninsula” and “At the Antarctic Ice shelves” should be changed to “On the...”

Thank you for the suggestion. We have chosen to keep the use of “at the...” throughout the text, as we use the preposition “at” to indicate a specific location, which we also feel is appropriate here.

6. Page 9 line 22+23: are there also more data gaps in the high slope areas that add to the inaccuracies over these regions? If so it would be worth adding the point.

This sentence refers to the evaluation of grid cells observed by CryoSat-2 (therefore no data gaps), which when measuring high slope areas and operating in Low Resolution Mode only, can range to the peaks of undulations, thereby under-sampling troughs. When we interpolate the small proportion of grid cells that are unobserved, reduced data coverage within the search radius can lead to higher interpolation errors, which we address in Section 3.2.

7. Figure 1 and figure 8: please remove the lines connecting the points as these are misrepresentative. Both these figures would be better as histograms rather than line graphs.

Thank you for this suggestion, we have changed both of these figures to bar plots.

8. In the figure legend for figure 2 I would add a point explaining the noticeable blue line where the mode changes from LRM and SARIn modes.

Thank you for this suggestion, we have added a sentence to the figure caption:

“At the mode mask boundary, where CryoSat-2 switches between LRM and SARIn operating modes, grid cells are predominantly derived from 2 km model fits, as there are a reduced number of elevation measurements available to constrain model fits at a resolution of 1 km.”

## **Anonymous Referee #2**

*However, to my opinion, since the paper is presenting another Antarctic DEM a more detailed analysis and comparison to existing DEMs is required. Especially the implications, reliability of the new method compared to widely used interpolation*

*methods is worth to investigate in more depth. E.g. a comparison with the cited CryoSat-2 DEM of Helm et.al. could be used to demonstrate if and where this new approach in combination with 6 times more data is performing better or has weaknesses. E.g. a difference plot between both CryoSat-2 DEMs over whole Antarctica would be very informative to see in which areas the DEMs differ.*

In our paper we present a comparison of our new DEM and three currently available DEMs against an independent airborne laser altimeter elevation dataset, which we feel is the most rigorous way of investigating the reliability and accuracy of each DEM. From this analysis we report a lower median and root mean squared elevation difference for the Antarctic ice sheet when comparing our CryoSat-2 DEM than those of the other currently available DEMs, which we believe already demonstrates the accuracy and validity of our approach.

We feel that differencing two individual DEMs will illustrate their respective differences, but will not provide any information regarding their individual performance, as it is not reasonable to make an initial assumption that one DEM is more accurate than the other (which all have an average reported accuracy on the metre scale). The IceBridge dataset is an independent dataset from a different sensor with a well-documented accuracy (at the centimetre scale), and is therefore, to our opinion, an appropriate dataset with which to evaluate the DEMs. In addition, when differencing individual DEMs it is necessary to resample one DEM to the posting of the other, which can introduce interpolation errors (please see our preliminary response to your review, posted on 30<sup>th</sup> November 2017).

*I have some concerns about the applied pixel fit method. Since the elevation is generated on a pixel level (neighboring pixel are not 'talking to each other'). This might introduce elevation jumps or artefacts. As example I generated hill shades of the new DEM and the mentioned external DEMs (Fig1). The new DEM shows clearly erroneous pixels, especially in areas of steep topography, close to the Grounding line. I'm wondering if the authors can explain why this is happening and if there is a strategy to avoid this. The other DEMs do not show such artefacts.*

As we have requested in our preliminary response to your comment (posted on 30<sup>th</sup> November 2017), could you please confirm the source of our DEM used to generate the figures in your review? Earlier this year we made a preliminary version of the CryoSat-2 DEM available for download to the community, which is posted at a coarser resolution of 2 km and not generated with the same blended approach as described in our manuscript. As such it is a separate product from the new 1 km CryoSat-2 DEM reported in this paper, which is not yet publicly available. We apologise for any confusion caused by this.

We feel the accuracy of our approach at a resolution of 1 km in areas of steep topography is well demonstrated in our evaluation against IceBridge measurements (Figure 7 and Table 2 in the manuscript). In Figure 8 of our manuscript we show our DEM is more accurate in areas of steep topography (e.g. Antarctic Peninsula) than the other available DEMs.

Previous DEMs generated from smaller time intervals and using an interpolation method applied to the entire ice sheet will still likely include these artefacts as they are in the data, but are harder to spot as a result of spatial smoothing. In addition, such smoothing introduces a spatial correlation across the search radius, degrading the resolution of the DEM beyond its stated posting value. We prefer that our primary product is posted at the true resolution of the data, and therefore is a true reflection of its quality. However, we will include a supplementary smoothed version of the DEM in our final release for any users who would prefer such a product, or they can easily apply a smoothing method of their own preference.

*In table 3 a comparison of the Differences of LRM/SARIn areas to Icebridge with respect to slope is given. Since the new DEM is a composite of 'observed pixels' and 'interpolated pixels' I would like to see this analysis splitted up (similar to Table 2).*

We feel the purpose of Table 3 is to illustrate that the uncertainty of observed grid cells increases with surface slope, and is one of the principal sources of the reported elevation differences when comparing CryoSat-2 to IceBridge. While the DEM is a composite of observed and interpolated pixels, the proportion of pixels that are interpolated only represent 5% of the total Antarctic ice sheet area. These interpolated grid cells predominantly occur at the Antarctic Peninsula, Transantarctic Mountains, and the Cook Mountains – areas of rugged terrain and slope greater than  $0.75^\circ$  (Figure 5). The analysis with respect to slope presented in Table 3 accounts for 95% of the total ice sheet area, and gives a good depiction of the accuracy of the overall product. We believe splitting up interpolated grid cells with respect to slope in the way suggested will not add anything to the description of the accuracy of interpolated grid cells, which we feel is sufficiently addressed in Section 3.2 and Table 2.

*Furthermore, I would suggest to present two figures where the mean difference and respectively the Stddev is plotted against slope (e.g. binned to 0.05) for the whole DEM, observed and interpolated pixel, respectively. In addition, this Figure should include the same analysis for the other 3 DEMs. Such kind of figure would clearly show the difference between observed and interpolated pixels as well as the stated improvement of the new DEM against existing DEMs.*

Thank you for this suggestion, however the IceBridge airborne dataset used in our study for evaluating the accuracy of DEMs preferentially samples areas of high slope (as stated in page 6, line 25). As such, we feel binning elevation differences as a function of slope in this way will not provide a robust indication of the accuracy of a DEM, as the slope distribution of the evaluation dataset is not representative of the slope distribution of the Antarctic ice sheet.

As submitted the manuscript already contains nine figures, of which four address the accuracy of our DEM. We believe this is already a large amount of figures, and that our manuscript already demonstrates the value of our DEM when compared to existing products.

*Is there a way to compare the final slope model (Fig 5) with the 2D quadratic surface slope, estimated for each pixel?*

From a comparison of the slopes from Figure 5 in the manuscript (estimated from the  $dz/dx$  and  $dz/dy$  components) and the modelled quadratic surface slopes in observed grid cells we generally find good agreement, with a mean and RMS difference of 0.04 and 0.5 degrees, respectively for the Antarctic ice sheet. However, it should be noted that this is not a fair like-for-like comparison – the modelled quadratic surface slopes represent the slope within the pixel, whilst the slopes in Figure 5 are the calculated from pixel to pixel, so we are comparing slopes estimated over different length scales here.

We realise when we introduced the slope from the DEM in the manuscript we were ambiguous in describing how it was generated; we have amended some text to make this clearer:

“Surface slopes derived from the elevation gradient of the DEM (Fig. 5) illustrate the short scale topographic undulations, and identify the ice divides and larger features such as subglacial Lake Vostok.”

*How robust is this pixel wise 2D surface fit and its sensitivity to the number and distribution of data points within a pixel? One could run the same fit method on yearly subsets of data and compare the elevations of 'observed pixels' of the subset DEMs with the Final DEM. (e.g. generate maps of the mean of the differences between subset-DEMs and final DEM and its stdev).*

While it is true that the surface fit is sensitive to the number and distribution of data points, this will apply to the accuracy of any DEM regardless of its generation method. This is why we have used the most complete data set available here. During the generation of the DEM we removed any poorly constrained fits with a low number of data points, or where the residuals of the modelled elevation and observations are large. Performing a comparison as suggested above will not incorporate the effects of temporal change into the statistics, making it difficult to draw any conclusions. Our chosen model has been established and evaluated within the literature (Smith et al., 2009; Moholdt et al., 2010; Flament and Rémy, 2012; McMillan et al, 2014; McMillan et al., 2016; Konrad et al., 2017). We believe we have already demonstrated the validity of our approach for deriving surface elevation from our evaluation against the IceBridge airborne altimetry.

*Please make clear what kind of data you are using as input. You mention that an OCOG retracker is used for LRM data but another retracker for SARIn. Please explain why and what are the consequences (e.g bias based on the different retracker).*

We describe the input data used to generate our DEM in good detail in Section 2.1 (page 2, line 18 to page 3, line 11). In LRM and SARIn CryoSat-2 is operating in different acquisition modes: as a traditional pulse limited altimeter in LRM, and as a SAR altimeter in SARIn mode. These modes produce different waveform shapes (Wingham et al. 2006), and as such it is appropriate to treat them with different retrackers, as we have here. We believe in this manuscript it is important to address the

absolute accuracy of the DEM, which we have done in detail. A relative intercomparison of different retrackerers is a separate body of work beyond the scope of this manuscript.

We have added a clause in Section 2.1 which addresses the use of different retrackerers:

“For the SARIn area, where CryoSat-2 operates as a SAR altimeter and waveform characteristics differ from those acquired in LRM, elevations are retrieved we using the ESA Level 2 SARIn retracker, which determines the retracking correction from fitting the measured waveform to a modelled SAR waveform (Wingham et al., 2006; ESA, 2012).”

*Are you applying any slope correction to the LRM data? If yes what method is used and which DEM is used for the slope correction? Do you use your newly derived DEM and an iterative scheme? If you use another DEM, please explain why. If you don't apply a slope correction to LRM than I see some inconsistency between the LRM and SARIn regions, since the SARIN data is slope corrected using the interferometric phase.*

The LRM measurements are slope corrected as part of the ESA Level 2 product. We provide the requested information on page 3, line 2. The slope correction in the Level 2 product is performed using an external DEM to relocate the echoing point away from nadir in accordance with the surface slope. Implementing an iterative slope correction scheme for LRM observations would require building a Level 1 processor, which is outside the scope of our study, but could be an avenue for future improvements. However, from our comparison of DEMs to the IceBridge airborne dataset (Figure 8), we demonstrate that our DEM has an improved accuracy in the Antarctic ice sheet over those that have been generated with an iterative slope correction scheme.

*Do you use all data points or do you run a pre-filtering to exclude erroneous data points before running the fit procedure? Are there any filtering approaches used after applying the pixel wise fit?*

A series of quality flags are included in the ESA L2 product, which are used for removing respective observations before the surface fit. After the fit procedure, we remove elevations from poorly constrained model fits (stated in page 3, line 22), through defining a series of quality filters in order to remove poorly constrained or unrealistic model fit solutions. These included controls on (i) the number of elevation estimates within a grid cell, and the length of the overall time series, (ii) any poorly constrained solution with a high root mean squared difference in the residuals between model fits and observations, or 1-sigma uncertainty of the elevation change estimates, and (iii) any model fit that resulted in an unrealistic elevation change or slope estimate.

We have created a new supplementary material document with a section that provides information on our filtering approach used after applying the model fit to the data, and included a reference to this supplementary material in the main text in Section 2.2.

*I also miss a map of uncertainty for whole Antarctica coming along with the DEM which would be required for ice sheet modelers.*

Thank you for the suggestion, we have generated an uncertainty map for a new supplementary material document which is derived from the RMS error of the fit in observed grid cells, and the kriging error in interpolated grid cells.

*P8 L30: Why are you not applying an elevation trend correction to the interpolated areas? This is inconsistent. You could easily generate an interpolated dhdt map to correct for elevation change in interpolated areas.*

Our estimation of surface elevation over a time period of 6 years requires consistently resolving both elevation and elevation rates from our model fit method. By definition, in areas where we don't have an elevation value, we don't have a rate of elevation change with which to correct the elevation differences. Although it would be possible to generate an interpolated dh/dt map, it would introduce further interpolation errors. Our current validation provides an upper bound of the estimate of the error in interpolated grid cells, which includes errors due to both interpolation and elevation change.

In addition, the small proportion (5%) of interpolated grid cells in our DEM predominantly occur in areas of bare rock and rugged terrain at the Antarctic Peninsula, Transantarctic Mountains, and the Cook Mountains, and not in the areas where appreciable elevation change is occurring (Figure 2 in the manuscript). We illustrate this by plotting the median difference of evaluated interpolated grid cells in ice velocity bands for the Antarctic ice sheet (please see Figure AC1), obtained from the MEaSURES dataset (Rignot et al., 2011). In interpolated grid cells, the elevation difference is highest in slow flowing areas and generally decreases with increasing ice velocity (used here as a proxy for elevation change in the absence of a comprehensive observational dataset of elevation change, which would of course be more appropriate). As such, when evaluating interpolated grid cells against IceBridge, we believe the elevation difference is mainly due to the interpolation error, and not due to the temporal difference between the two estimates.

We have amended the text in the manuscript to make this clearer:

“We note that, because the elevation rate is unknown where there is no model solution, we have not corrected for temporal changes in elevation between the acquisition periods of the two datasets within our evaluation of interpolated grid cells. As a



result, the reported values represent an upper bound of the elevation difference which includes errors due to both interpolation and elevation change — if present within an interpolated grid cell.”

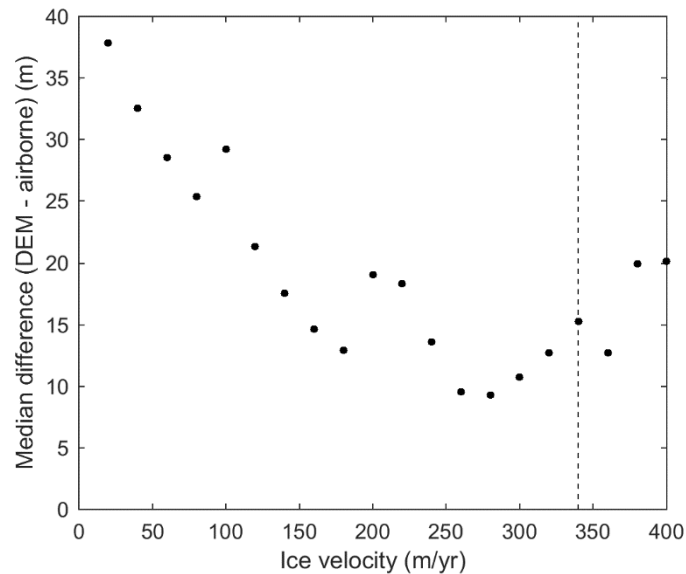


**Figure AC1: Median difference of interpolated DEM grid cells in the Antarctic ice sheet evaluated against IceBridge airborne measurements, binned into ice velocity bands 20 m/yr in size. 90% of all interpolated DEM grid cells in the Antarctic ice sheet are located in regions flowing slower than 340 m/yr, shown in the vertical dashed line.**

*Fig 8: Why is the median difference below zero in all cases - this would mean that CryoSat is measuring above the laser surface?*

All presented elevation differences are DEM - IceBridge (stated in page 5, line 22), therefore a negative elevation difference indicates that CryoSat-2 is measuring below the laser surface. This is within expectations – the Ku band operating frequency of CryoSat-2 will penetrate beyond a dry ice sheet surface into the snow pack, whereas the laser altimeter on-board IceBridge survey craft will return from the air-snow interface.

*Figures (2,3,4,5,6,7,9): please use km instead of m and overplot a Latitude / Longitude grid on top of the polarstereo projection.*

Thank you for this suggestion, we have added a latitude and longitude grid to the figures.

*Furthermore, I think that the new DEM is shifted by 1 pixel. Difference plots as suggested above show a strange pattern (see Fig. 2) which is not observed between the other 3 DEMs - Do you have any explanation?*

Please see our preliminary response to your review posted on 30<sup>th</sup> November 2017 regarding this comment, where we have addressed this in more detail.

### **Anonymous Referee #3**

#### **Sect 2.1**

*p.3, l. 8. Both references here are from before the launch of CS-2. It would be nice to back up this statement of the performance of the OCOG with literature that actually is based on CS-2 data, if possible.*

Thank you for this suggestion, we have also added a reference which highlights the use of the OCOG algorithm with CryoSat-2 data.

*p.3, l. 9-11. It is unclear to me if the authors use the L2 SARIn product from ESA or whether they perform the retracking themselves. In the case of the latter (which I suspect is the case) some more detail about the retracking algorithm should be added, in the same way as they describe the OCOG.*

Yes, we have used the ESA L2 SARIn product, please see Section 2.1 (page 2, line 18). Accordingly, we include the relevant citations which describe the algorithm in full detail, if the reader wishes to know more (page 3, line 10). We have also amended some wording in Section 2.1 to make clear the L2 product includes retracked elevations:

“Within the LRM mode mask area we select Level 2 elevation estimates retrieved using the Offset Centre of Gravity (OCOG) retracking algorithm (Wingham et al., 1986), which defines a rectangular box around the centre of gravity of an altimeter waveform based upon its power distribution (Wingham et al., 1986).”

“For the SARIn area, where CryoSat-2 operates as a SAR altimeter and waveform characteristics differ from those acquired in LRM, elevations are retrieved we using the ESA Level 2 SARIn retracker, which determines the retracking correction from fitting the measured waveform to a modelled SAR waveform (Wingham et al., 2006; ESA, 2012).”

#### **Sect 2.2**

*p.3, Eq.1. The model includes a  $t$ -term taking into account any trend in surface elevation in the grid cell. But some regions must also include an acceleration ( $t^2$  term). How will it affect the  $z$  value in a grid cell if an acceleration is present but not modelled?*

For our DEM elevation we select the mean elevation parameter,  $\bar{z}$ , which represents the elevation at the centre of our chosen time window, which will be insensitive to higher order terms in time. Our approach, which models the surface evolution over time, represents an evolution in the generation of DEMs, allowing the use of longer observation periods.

In addition, recorded regions where acceleration has occurred are rare in Antarctica (Konrad et al., 2017) – the surface elevation of the majority of the continent is either not changing, or changing linearly with time. Any acceleration over our 6-year observation period will not be occurring fast enough to warrant accounting for in our modelled solution. Our chosen model is well established and evaluated in the literature to accurately capture elevation change (Smith et al., 2009; Moholdt et al., 2010; Flament and Rémy, 2012; McMillan et al, 2014; McMillan et al., 2016). Finally, adding more terms will make our model fit more unstable. Because of this, and the points above, we feel our use of a linear rate of elevation change is appropriate here.

*p.3, l. 22. What is your definition of “unrealistic estimates”?*

This comment was also raised by Anonymous Referee #2, please find our response duplicated below:

A series of quality flags are included in the ESA L2 product, which are used for removing respective observations before the surface fit. After the fit procedure, we remove elevations from poorly constrained model fits (stated in page 3, line 22), through defining a series of quality filters in order to remove poorly constrained or unrealistic model fit solutions. These included controls on (i) the number of elevation estimates within a grid cell, and the length of the overall time series, (ii) any poorly constrained solution with a high root mean squared difference in the residuals between model fits and observations, or 1-sigma uncertainty of the elevation change estimates, and (iii) any model fit that resulted in an unrealistic elevation change or slope estimate.

We have created a new supplementary material document with a section that provides information on our filtering approach used after applying the model fit to the data, and included a reference to this supplementary material in the main text in Section 2.2.

*p.3, l. 29-30. The method results in 60% of the 1km grid cells on the ice sheet and 75% on the ice shelves having  $z$  values. Is this due to lack of measurements in the remaining grid cells? What is the minimum number of data that you require to provide a  $z$ -value in a grid cell? And do you have a requirement on the time span that must be covered by available measurements?*

Correct, elevations were derived from 2 km and 5 km model fits when there was an insufficient number of elevation measurements to accurately constrain model fits at the finer grid cell resolutions of 1 km and 2 km, respectively. We discarded any model fit elevations that were derived from less than 15 measurements, or a time series of less than 2 years in length. This information is now available in the previously mentioned supplementary material document, where we describe our data filtering approach in more detail.

*Also, have the authors performed relocation (due to topography) of the LRM data, and if so, how is this done? This should be clarified.*

The LRM measurements are slope corrected as part of the ESA Level 2 product, please see page 3, line 2. The slope correction for LRM measurements is performed using an external DEM to relocate the echoing point in accordance with the slope. More information is available to the reader through the cited literature.

### **Sect 3**

*I think that some of the information provided in this section actually fits better under Sect 2.4 (DEM evaluation), e.g. what statistics are being derived, how to account for elevation changes etc.*

Thank you for your suggestion – we feel this information is equally valid in either section, and have chosen to keep it in Section 3. Because the majority of the results reported are in terms of these statistics, we believe it is appropriate to include it in Section 3, in terms of making it easier to follow for the reader. When accounting for elevation changes, we only do so in observed regions, so we feel this information is most appropriate in the section which addresses observed grid cells.

*p. 6, l. 16 Isn't it the case that when using Eq. 1 to find the elevation ( $z$ ) in a grid cell, this elevation actually corresponds to the elevation at  $t=0$ , meaning 2010 (or whatever the start time of measurements in the grid cell is)? Did you ensure the effective time stamp to be July 2013 by defining this to be  $t=0$ ?*

When forming the DEM we do not use the modelled elevation  $Z$ , we use the mean elevation parameter  $\bar{z}$ , which is representative of the elevation at the midpoint of the elevation time series. We believe that Table 1 and Figure 6 evidence that the DEM timestamp is indeed July 2013. We have also adjusted equation 1 and amended the text to make it clear to the reader that  $\bar{z}$  corresponds to the elevation at July 2013, which is the midpoint of our observation period:

“We form the DEM from the mean elevation term,  $\bar{z}$ , in Eq. (1) within each 1 x 1 km grid cell, which corresponds to the elevation at the midpoint of our observation period.”

### **Sect 3.1**

*p. 6, l. 15-17 Yes, but this is only the case if the time stamp is actually July 2013 (see my previous comment).*

Please see our response to your previous comment regarding the effective time stamp of the DEM.

*p. 6, l. 31-33. Why didn't you correct for the temporal elevation changes here?*

Please note in addressing this comment we are assuming you are referring to page 8, lines 31-33 in Section 3.2, and our choice to not correct for elevation change when evaluating interpolated grid cells. This was also raised by Anonymous Referee #2, please find our response duplicated below:

Our estimation of surface elevation over a time period of 6 years requires consistently resolving both elevation and elevation rates from our model fit method. By definition, in areas where we don't have an elevation value, we don't have a rate of elevation change with which to correct our elevation differences. Although it would be possible to generate an interpolated  $dh/dt$  map, it would introduce further interpolation errors. Our current validation provides an upper bound of the estimate of the error in interpolated grid cells, which includes errors due to both interpolation and elevation change.

In addition, the small proportion (5%) of interpolated grid cells in our DEM predominantly occur in areas of bare rock and rugged terrain at the Antarctic Peninsula, Transantarctic Mountains, and the Cook Mountains, and not in the areas where appreciable elevation change is occurring (Figure 2 in the manuscript). We illustrate this by plotting the median difference of evaluated interpolated grid cells in ice velocity bands for the Antarctic ice sheet (please see Figure AC1), obtained from the MEaSURES dataset (Rignot et al., 2011). In interpolated grid cells, the elevation difference is highest in slow flowing areas and generally decreases with increasing ice velocity (used here as a proxy for elevation change in the absence of a comprehensive observational dataset of elevation change, which would of course be more appropriate). As such, when evaluating interpolated grid cells against IceBridge, we believe the elevation difference is mainly due to the interpolation error, and not due to the temporal difference between the two estimates.

We have amended the text in the manuscript to make this clearer:

“We note that, because the elevation rate is unknown where there is no model solution, we have not corrected for temporal changes in elevation between the acquisition periods of the two datasets within our evaluation of interpolated grid cells. As a result, the reported values represent an upper bound of the elevation difference which includes errors due to both interpolation and elevation change — if present within an interpolated grid cell.”

## Figures

*Figure 6. The colour scale is not optimal. First thing is that all the differences shown all look blue/green, making it difficult to see if there are any local differences. Also, the colours of the max and min values in the colour scale look similar (to me at least).*

*Figure 7. Same comment as for figure 6.*

Agreed, thank you for this suggestion. We have changed the colour scale for the difference plots to a divergent one, which we hope makes them easier to read.

## References

Flament, T. and Rémy, F.: Dynamic thinning of Antarctic glaciers from along-track repeat radar altimetry, *J. Glaciol.*, 58, 830–840, doi:10.3189/2012JoG11J118, 2012.

Konrad, H., Gilbert, L., Cornford, S.L., Payne, A., Hogg, A., Muir, A., and Shepherd, A., Uneven onset and pace of ice dynamical imbalance in the Amundsen Sea Embayment, West Antarctica, *Geophys. Res. Lett.*, 44, 910–918, 2017.

McMillan, M., Shepherd, A., Sundal, A., Briggs, K., Muir, A., Ridout, A., Hogg, A., and Wingham, D.: Increased ice losses from Antarctica detected by CryoSat-2, *Geophys. Res. Lett.*, 41, 3899–3905, doi:10.1002/2014GL060111, 2014GL060111, 2014.

McMillan, M., Leeson, A., Shepherd, A., Briggs, K., Armitage, T. W. K., Hogg, A., Kuipers Munneke, P., van den Broeke, M., Noël, B., van de Berg, W. J., Ligtenberg, S., Horwath, M., Groh, A., Muir, A., and Gilbert, L.: A high-resolution record of Greenland mass balance, *Geophys. Res. Lett.*, 43, 7002–7010, doi:10.1002/2016GL069666, 2016.

Rignot, E., Mouginot, J., and Scheuchl, B.: Ice Flow of the Antarctic Ice Sheet, *Science*, 333, 1427–1430, doi:10.1126/science.1208336, 2011.

Moholdt, G., Nuth C., Hagen J. O., and Kohler J.: Recent elevation changes of Svalbard glaciers derived from ICESat laser altimetry, *Remote Sens. Environ.*, 114(11), 2756–2767, doi:10.1016/j.rse.2010.06.008, 2010.

Smith, B. E., Fricker H. A., Joughin, I. R., and Tulaczyk S.: An inventory of active subglacial lakes in Antarctica detected by ICESat (2003–2008), *J. Glaciol.*, 55(192), 573–595, doi:10.3189/002214309789470879, 2009.

Wingham, D., Francis, C. R., Baker, S., Bouzinac, C., Cullen, R., de Chateau-Thierry, P., Laxon, S. W., Mallow, U., Mavrocordatos, C., Phalippou, L., Ratier, G., Rey, L., Rostan, F., Viau, P., and Wallis, D.: CryoSat: a mission to determine the fluctuations in Earth's land and marine ice fields, *Adv. Space Res.*, 37, 841–871, doi:10.1016/j.asr.2005.07.027, 2006.

# A new Digital Elevation Model of Antarctica derived from CryoSat-2 altimetry

Thomas Slater<sup>1</sup>, Andrew Shepherd<sup>1</sup>, Malcolm McMillan<sup>1</sup>, Alan Muir<sup>2</sup>, Lin Gilbert<sup>2</sup>, Anna E. Hogg<sup>1</sup>, Hannes Konrad<sup>1</sup>, Tommaso Parrinello<sup>3</sup>

5 <sup>1</sup>Centre for Polar Observation and Modelling, School of Earth and Environment, University of Leeds, Leeds, LS2 9JT, United Kingdom

<sup>2</sup>Centre for Polar Observation and Modelling, University College London, London, WC1E 6BT, United Kingdom

<sup>3</sup>ESA ESRIN, Via Galileo Galilei, 00044 Frascati RM, Italy

*Correspondence to:* Thomas Slater ([py10ts@leeds.ac.uk](mailto:py10ts@leeds.ac.uk))

## 10 **Abstract.**

We present a new Digital Elevation Model (DEM) of the Antarctic ice sheet and ice shelves based on  $2.5 \times 10^8$  observations recorded by the CryoSat-2 satellite radar altimeter between July 2010 and July 2016. The DEM is formed from spatio-temporal fits to elevation measurements accumulated within 1, 2 and 5 km grid cells, and is posted at the modal resolution of 1 km. Altogether, 94 % of the grounded ice sheet and 98 % of the floating ice shelves are observed, and the remaining grid cells  
15 North of  $88^\circ\text{S}$  are interpolated using ordinary kriging. The median and root mean square difference between the DEM and  $2.3 \times 10^7$  airborne laser altimeter measurements acquired during NASA Operation IceBridge campaigns are -0.30 m and 13.50 m, respectively. The DEM uncertainty rises in regions of high slope — especially where elevation measurements were acquired in Low Resolution Mode — and, taking this into account, we estimate the average accuracy to be 9.5 m — a value that is comparable to or better than that of other models derived from satellite radar and laser altimetry.

## 20 **1 Introduction**

Digital Elevation Models (DEMs) of Antarctica are important datasets required for the planning of fieldwork, numerical ice sheet modelling, and the tracking of ice motion. Measurements of ice sheet topography are needed as a boundary condition for numerical projections of ice dynamics and potential sea level contributions (Cornford et al., 2015; Ritz et al., 2015). Accurate knowledge of surface elevation ~~can be used is also essential~~ for both the delineation of drainage basins and estimation of  
25 grounding line ice thickness, necessary for estimates of Antarctic mass balance calculated via the mass budget method (Rignot et al., 2011b; Shepherd et al., 2012; Sutterly et al., 2014). Furthermore, detailed and up-to-date DEMs are required to distinguish between phase differences caused by topography and ice motion when estimating ice velocity using interferometric synthetic aperture radar (Rignot et al., 2011a; Mouginot et al., 2012).



Previously published DEMs of Antarctica have been derived from satellite radar altimetry (Helm et al., 2014, Fei et al., 2017), laser altimetry (DiMarzio et al., 2007), a combination of both radar and laser altimetry (Bamber et al., 2009; Griggs and Bamber, 2009), and through the integration of several sources of remote sensing and cartographic data (Liu et al., 2001; Fretwell et al., 2013). In addition, high resolution regional DEMs of the marginal areas of the ice sheet have been generated from stereoscopic (Korona et al., 2009) and radiometer surveys (Cook et al., 2012). ~~However~~ Although these photogrammetric models perform well over regions of bare rock and steep slope found in the margins, ~~the accuracy of both of these remote sensing techniques~~ their accuracy is considerably reduced in ice covered areas.

CryoSat-2, launched in 2010, is specifically designed to overcome the challenges of performing pulse-limited altimetry over Earth's polar regions. With a high inclination, drifting orbit, and novel instrumentation which exploits interferometry to obtain high spatial resolution measurements in areas of steep terrain, CryoSat-2 provides a high density network of elevation measurements up to latitudes of 88 ° (Wingham et al., 2006). Here, we utilise a ~~6-year~~ 6-year time series of elevation measurements acquired by CryoSat-2 between July 2010 and July 2016 to derive a comprehensive and contemporary DEM of Antarctica at a spatial resolution of 1 km, with high data coverage in both the ice sheet interior and its complex marginal areas. We then evaluate the accuracy of the generated DEM against a set of contemporaneous airborne laser altimeter measurements, obtained during NASA Operation IceBridge campaigns, in several locations covering Antarctica's ice sheet and ice shelves.

## 2 Data and methods

### 2.1 CryoSat-2 elevation measurements

We use 6 years of CryoSat-2 Baseline-C Level 2 measurements of surface elevation recorded by the SIRAL (SAR Interferometer Radar Altimeter) instrument, mounted on the CryoSat-2 satellite, between July 2010 and July 2016. Over Antarctica, SIRAL samples the surface in two operating modes: Low Resolution Mode (LRM) and Synthetic Aperture Radar Interferometric mode (SARIn). In LRM, Cryosat-2 operates as a conventional pulse-limited altimeter (Wingham and Wallis, 2010), illuminating an area of approximately 2.2 km<sup>2</sup>, with an across track width of roughly 1.5 km. LRM is used in the interior of the ice sheet, where low slopes and homogenous topography on the footprint scale are generally well suited for pulse-limited altimetry.

In SARIn, SIRAL uses two receive antennae to perform interferometry, allowing the location of the point of closest approach (POCA) to be precisely determined in the across-track plane (Wingham et al., 2004). ~~In SARIn mode,~~ bursts of 64 pulses are emitted at a high Pulse Repetition Frequency, and Doppler processing is then used to reduce the along-track footprint to approximately 300 m (Wingham et al., 2006). This increased sampling density, and ability to calculate the along- and across-track location of the POCA, make SARIn well suited for measuring the steep and complex topography found in the ice sheet margins.

The CryoSat-2 Level 2 elevation product has a series of geophysical corrections applied to correct the selected measurements for the following: off-nadir ranging due to slope, dry atmospheric propagation, wet atmospheric propagation, ionosphere propagation, solid earth tide and ocean loading tide (ESA, 2012). For the ice shelves, additional inverse barometric and ocean tide corrections are also applied. Within the LRM mode mask area we ~~use~~ select Level 2 elevation estimates retrieved using the Offset Centre of Gravity (OCOG) retracking algorithm (Wingham et al., 1986) to retrieve the L2 elevation estimates, which defines a rectangular box around the centre of gravity of an altimeter waveform based upon its power distribution (Wingham et al., 1986). The OCOG retracking point is taken to be the point on the leading edge of the waveform which first exceeds 30 % of the rectangle's amplitude (Davis, 1997). We ~~select~~ use the OCOG retracker as it offers robust retracking over a wide range of surfaces, and is adaptable to a variety of pulse shapes (Wingham et al., 1986; Davis, 1997; Armitage et al., 2013). For the SARIn area, where CryoSat-2 operates as a SAR altimeter and waveform characteristics differ from those acquired in LRM, elevations are retrieved we using the ESA Level 2 SARIn retracker, which determines the retracking correction from fitting the measured waveform to a modelled SAR waveform (Wingham et al., 2006; ESA, 2012). Over the ice sheet and ice shelves, we use approximately  $2.5 \times 10^8$  CryoSat-2 elevation measurements to derive the new DEM.

## 15 2.2 DEM generation

To compute elevation, we separate the input CryoSat-2 elevation measurements into approximately  $1.4 \times 10^7$  regularly spaced  $1 \text{ km}^2$  geographical regions. We then use a model fit method to separate the various contributions to the measured elevation fluctuations within each region (Flament and Remy, 2012; McMillan et al., 2014). This method best suits CryoSat-2's 369-day orbit cycle, which samples along a dense network of ground tracks with few coincident repeats. We model the elevation  $Z$ ; (Eq. (1)); as a quadratic function of local surface terrain  $(x,y)$ , a time invariant term  $h$  accounting for anisotropy in radar penetration depth depending on satellite direction (Armitage et al., 2013), and a linear rate of elevation change with time  $t$ . The satellite heading term,  $h$ , is a binary term set to 0 or 1 for an ascending or descending pass, respectively.

$$Z(x, y, t, h) = \bar{z} + a_0x + a_1y + a_2x^2 + a_3y^2 + a_4xy + a_5(h) + a_6(t - t_{July\ 2013}) \quad (1)$$

25 We retrieve the model coefficients in each grid cell using an iterative least-squares fit to the observations to minimise the impact of outliers, and discard unrealistic estimates resulting from poorly constrained model fits (see supplementary material). At a spatial resolution of  $1 \text{ km}$  this approach provides, on average, in excess of 30 elevation measurements per grid cell to constrain each solution. By using the model fit method, we are able to generate elevation estimates from 6 years of continuous Cryosat-2 data, which are not unduly affected by fluctuations in surface elevation that may occur during the acquisition period  
30 (McMillan et al., 2014). In addition, it also allows for the retrieval of ice sheet elevation and rate of elevation change from the same data in a self-consistent manner.

We form the DEM from the mean elevation term,  $\bar{z}$ , in Eq. (1) within each 1 x 1 km grid cell, which corresponds to the elevation at the midpoint of our observation period. At a resolution of 1 km, the model fit provides an elevation estimate in 60 % and 75% of grid cells within the ice sheet, and 75 % in the ice shelves within the total area of the ice sheet and ice shelves, respectively. To fill data gaps in the 1 km grid, we generate additional DEMs of Antarctica from model fits at spatial resolutions of 2 km and 5 km. At these coarser resolutions more data are available to constrain model fits within a given geographical region, particularly at lower latitudes where the spacing between ground tracks is larger. As a result, ~~forever~~ the ice sheet the data coverage for DEMs generated at resolutions of 2 km and 5 km is increased to 91 % and 94 %, respectively (Fig. 1). For the ice shelves we use an additional DEM generated from model fits at a resolution of 2 km, for which data coverage is increased to 98 %. Data gaps in the 1 km grid are filled by the re-sampled 2 km and 5 km DEMs (where neither 1 km or 2 km model fit estimates are available) for the ice sheet, and the 2 km DEM for the ice shelves (Fig. 2). This approach provides a DEM at the modal spatial resolution of 1 km, where approximately 94 % and 98 % of grid cells contain an elevation estimate derived from CryoSat-2 measurements for the ice sheet and ice shelves, respectively.

In order to provide a continuous dataset, we estimate elevation values in grid cells North of 88 ° S that contain no data using ordinary kriging (Isaaks and Srivastava, 1989; Kitanitis 1997), an interpolation technique used in the generation of previously published DEMs (Bamber et al., 2009; Helm et al., 2014).- We interpolate using ~~with~~ a search radius of 10, 25 or 50 km, depending on which first satisfies a minimum threshold of 100 data points to be used in the interpolation. Over the grounded ice sheet, 44 %, 52 % and 4 % of interpolated elevation values used a search radius of 10, 25 and 50 km, respectively. The majority of data points requiring a search radius of 50 km are located along the margins of Graham Land and Palmer Land in the Antarctic Peninsula, where data coverage is poor. After interpolation, the DEM provides a continuous elevation dataset for the ice shelves and ice sheet for latitudes north of 88-° S-S. We have chosen not to interpolate the pole hole due to interpolation distances exceeding the maximum kriging search radius of 50 km, and a desire to keep the DEM a product of CryoSat-2 data only.

### 2.3 Airborne elevation measurements

To evaluate the accuracy of the DEM, we compare our elevation estimates to measurements acquired by airborne laser altimeters during NASA's Operation IceBridge survey. The IceBridge mission, running since 2009, is the largest airborne polar survey ever undertaken (Koenig et al., 2010). The primary goal of IceBridge is to maintain a continuous time series of laser altimetry over the Arctic and the Antarctic, bridging the gap between ICESat, which stopped collecting data in 2009, and ICESat-2, planned for launch in 2018.

We compare the DEM to elevation measurements obtained by two airborne laser altimeter instruments (Fig. 3):

- The Airborne Topographic Mapper (ATM), over the following regions of the continental ice sheet: Antarctic Peninsula, Bellingshausen, Amundsen and Getz sectors of West Antarctica, and the Transantarctic Mountains, Oates

Land and the plateau region of East Antarctica. The following ice shelves were also surveyed: Larsen C, Pine Island, Thwaites, Wilkins, Abbot, Getz, George VI, Ross and Filchner-Ronne. Measurements were acquired between March 2009 and December 2014 (Krabill, 2016).

- The Riegl Laser Altimeter (RLA), over the Antarctic Peninsula, Marie Byrd Land of West Antarctica, Dronning Maud Land, Totten Glacier and Wilkes Land of East Antarctica, and the Ross ice shelf. Measurements were acquired between December 2008 and January 2013 (Blankenship et al., 2013).

The ATM is an airborne scanning laser altimeter capable of measuring surface elevation with an accuracy of 10 cm or better (Krabill et al 2004). Flown at a typical altitude of 500 m above ground level, the ATM illuminates a swath width of approximately 140 m, with a footprint size of 1-3 m and along track separation of 2 m (Levinsen et al., 2013). Data acquired by the RLA were collected as part of the NASA ICECAP program from December 2009 to 2013, mounted to a survey aircraft flown at a typical height of 800 m. Elevation measurements are provided at a spatial resolution of 25 m along track and 1 m across track with an error of approximately 12 cm (Blankenship et al., 2013).

In total, we selected approximately  $2.3 \times 10^7$  laser altimeter elevation measurements, comprising of  $1.7 \times 10^7$  ATM measurements, and  $0.6 \times 10^7$  RLA measurements. Combined, these data provide an independent comparison dataset, obtained over a contemporaneous time period and in a wide range of locations across Antarctica. For all airborne measurements, a filter was applied to remove any erroneous step changes in elevation resulting from the laser altimeter ranging from cloud cover (Young et al., 2008; Kwok et al., 2012).

## 2.4 DEM evaluation

When comparing the DEM and airborne laser altimeter datasets, we separate the evaluation results according to whether the IceBridge elevation measurement resides in a grid cell derived from CryoSat-2 surface height measurements, hereby referred to as an observed grid cell, or an interpolated elevation value. This approach allows the accuracy of CryoSat-2 observations and the chosen interpolation method to be assessed independently. In total, approximately 84 % of the airborne laser elevation measurements reside within an observed DEM grid cell. Of this total, 53 %, 41 % and 6 % grid cells are derived from 1, 2 and 5 km model fits, respectively.

In order to compare the DEM and IceBridge datasets, we estimate the DEM elevations at the exact location of the airborne laser altimeter measurement through bilinear interpolation. Subsequently, we subtract the IceBridge elevation from the interpolated DEM elevation and collate the elevation differences into the same 1 x 1 km grid that the DEM is projected on. We then calculate the median difference to obtain one elevation difference for each individual grid cell, and to minimise the impact of outliers. On average, 1 km DEM grid cells overflown by IceBridge campaigns contain 70 individual airborne

measurements. In total, elevation differences were compared for approximately  $2.7 \times 10^5$  DEM grid cells, covering 2 % of the total ice sheet and ice shelf area, respectively. All DEM and IceBridge elevations are referenced to the WGS84 ellipsoid.

### 3 Results

Our new DEM of Antarctica (Fig. 4) provides an elevation value derived from CryoSat-2 measurements for 94 % of the grounded ice sheet and 98 % of the ice shelves. The remaining 5 % of grid cells North of  $88^\circ\text{S}$  are interpolated using ordinary kriging to provide a continuous gridded elevation dataset for the entire continent beyond the pole hole. Accounting for the length of the elevation time series within each individual grid cell, we determine the effective time stamp of the DEM to be July 2013. Surface slopes derived from the [elevation gradient of the DEM](#) (Fig. 5) illustrate the short scale topographic undulations, and identify the ice divides and larger features such as subglacial Lake Vostok.

To evaluate the DEM's systematic bias we compute the median elevation difference with respect to the airborne measurements, as this is robust against the effect of outliers. To evaluate its random ~~error~~[error](#), we ~~compute~~[calculate](#) the root mean square (RMS) difference. Both of these statistical measures are more appropriate [than the mean and standard deviation](#) when describing the systematic bias and random error, respectively, of the non-Gaussian distributions we typically find when calculating elevation differences between the DEM and IceBridge elevation datasets.

#### 3.1 Comparison of DEM to airborne elevation measurements: observed grid cells

A primary objective of NASA's IceBridge program is to maintain a continuous observational record of rapidly changing areas in Antarctica. As a result, elevation measurements were obtained in regions such as Pine Island (PIG), Thwaites and Totten Glaciers, where the observed thinning rate is of the order of several metres per year (McMillan et al., 2014). Therefore, we expect to see height differences between the DEM and airborne datasets due to real changes in surface elevation between their respective acquisition periods. Comparing DEM elevations at PIG against measurements acquired by ATM flights in the years 2009, 2011 and 2014 (Fig. 6), the elevation difference is smallest in 2014, closest to the DEM effective date of July 2013 (Table 1).

To account for the temporal difference between the two datasets, we adjust the interpolated DEM value for changes in surface elevation which may have occurred between the acquisition periods. We calculate this adjustment by interpolating the gridded elevation trends (Eq. (1)) to the location of the airborne measurement, through the same bilinear interpolation method as used for the DEM elevation estimate. The elevation change trends were corrected for temporal fluctuations in backscattered power, which can introduce spurious signals in time series of elevation change (Davis and Ferguson, 2004; Khvorostovsky, 2012).

Within the grounded ice sheet, we note that the spatial distribution of the airborne dataset used for comparison (Fig. 7) preferentially samples regions of high slope and low elevation, and does not reflect the overall elevation and slope distributions of the Antarctic ice sheet. Approximately 60 % of DEM grid cells overflowed by IceBridge survey craft have an elevation of less than or equal to 1000 m, and 43 % have a surface slope greater than 0.5 °. In comparison, approximately 15 % and 22 % of the Antarctic ice sheet area has elevations of less than 1000 m and slopes greater than 0.5 °, respectively. At the continental scale, there is generally good agreement between the DEM and airborne laser altimeter measurements (Fig. 8), and the median and RMS elevation difference between the DEM and airborne data are -0.27 m and 13.36 m., respectively (Table 2).

At the Antarctic Peninsula, the median and RMS difference are -1.12 m and 22.40 m, respectively; errors are larger in this region due to its mountainous and highly variable terrain, and it remains a challenge for radar altimetry. The largest elevation differences in this region are found in DEM grid cells derived from 5 km model fits, indicating that the complex topography is poorly described by a quadratic model at this resolution. In grid cells with elevation values derived from 1 km model fits, which accounts for 40 % of the Antarctic Peninsula DEM, the median and RMS difference are improved to -0.71 m and 16.88 m, respectively. Geographically, elevation differences rise towards Graham Land at the northern tip of the Antarctic Peninsula, where topography is complex and highly variable at length scales similar to the satellite footprint.

In West Antarctica there is good agreement between the DEM and airborne measurements, particularly along the coastal margins of the Bellingshausen and Amundsen Seas. In the Bryan and Eights Coasts in the Bellingshausen Sea Sector, the median and RMS difference are -1.72 m and 10.40 m, respectively. At Pine Island and Thwaites Glaciers, and their surrounding drainage area, the median difference is -1.02 m, and the RMS difference is 10.58 m. Further inland towards Marie Byrd Land, the median and RMS differences are 0.20 m and 5.27 m, respectively.

In East Antarctica, the DEM compares well to the airborne dataset inland in the plateau region where slopes are low, and the topography is well suited to satellite radar altimetry. Along the George coast and in George V Land, the median difference is -0.68 m, and the RMS difference 6.52 m. Over Totten glacier and its catchment area, the median and RMS difference are -0.39 m and 16.15 m respectively. In this region, there is good agreement with airborne elevations both inland towards Dome C, and over Totten glacier itself. On the eastern flank of Law Dome, biases of several tens of metres between the DEM and the airborne data coincide with grid cells derived from 5 km model fits, where there is insufficient data to constrain models at higher spatial resolutions. As a result, elevations derived from 5 km model fits will poorly sample the highly sloping terrain in this region when compared to the airborne laser. Additionally, in East Antarctica, elevation differences several tens of metres in magnitude over the Pensacola Mountains occur where high surface slopes and nunataks complicate radar altimeter elevation retrievals.

At the Antarctic ice shelves, the DEM also compares favourably to the airborne elevation data, with median and RMS differences of -0.42 m and 14.31 m, respectively. Differences are most pronounced near to grounding lines where tidal effects are relatively large and where the terrain is generally more complex, and are smallest in the interior of the larger ice shelves, which are generally flat. At the Ross and Filchner-Ronne Ice Shelves, for example, the RMS differences are 3.93 and 3.54 m, respectively — considerably lower than the continental average.

Overall, the median and RMS differences between the DEM and airborne measurements are -0.30 m and 13.50 m, respectively, and 99 % of the data agree to within 45 m. In addition to temporal mismatch, possible explanations for residual elevation differences include differences in the satellite and airborne altimeter footprint sizes and scattering horizons, as well as errors in the individual data sets themselves. Although generally small, biases between the DEM and the airborne data are notably high in several isolated regions, including the upstream catchments of the Byrd Glacier flowing from East Antarctica into the Ross Ice Shelf, the Recovery Glacier flowing from East Antarctica into the Filchner Ice Shelf, and the Foundation Ice Stream in the Pensacola mountains (see Fig. 7). In each of these locations, surface slopes are high (exceeding 1 °) and CryoSat-2 operates in Low Resolution Mode (see Fig. 5). To illustrate this in more detail, we compare elevation recorded along two RLA tracks falling within the LRM zone (Fig. 9); one at Byrd Glacier where slopes are high and undulating, and another 600 km northward in Victoria Land where slopes are low and smooth. Along these tracks, elevation differences of approximately 20 m occur where the terrain undulates rapidly, because CryoSat-2 ~~oversamples the topography~~undersamples the topographic depressions when operating in LRM. Despite being well sampled by the airborne laser altimeter dataset, regions of high surface slopes represent a small fraction of the area surveyed by CryoSat-2 in either LRM or SARIn modes (Table 3). In contrast, agreement between DEM and IceBridge elevations in regions of lower surface slope ( $< 0.5^\circ$ ) — which represent the majority of the ice sheet — falls typically in the range 5 to 10 m in either operating mode (Table 3). Combining the slope-dependent errors (Table 3) and the distribution of slopes within the LRM and SARIn mode masks, we estimate the average uncertainty of the observed DEM to be 9.5 m.

### 3.2 Comparison of DEM to airborne elevation measurements: interpolated grid cells

A small proportion (5 %) of the DEM is estimated by ordinary kriging, and we assess the accuracy of this method by comparing airborne elevation measurements residing in a DEM grid cell containing no data with the interpolated value (Table 2). Predictably, our interpolated DEM values deviate more from the airborne elevation measurements in areas of high slope and complex terrain, where internal tracker losses occur and data coverage is reduced. This is true in particular for the ice sheet margins and the Antarctic Peninsula, where there is little spatial correlation over the 10, 25 and 50 km search distances we have chosen for the interpolation, and limited data coverage available for sampling. At the Antarctic Peninsula, where the majority of interpolated grid cells are located in the bare rock regions on the north coasts of Graham and Palmer Land, the median and RMS difference are 82.21 m and 191.07 m, respectively. ~~Similarly~~Similarly, in East Antarctica, where the median

and RMS difference are 19.62 m and 117.77 m, respectively, interpolated grid cells are primarily found in the rugged, bare rock terrain across the Transantarctic Mountains, the Victory Mountains in Victoria Land, and the mountain ranges in Oates Land.

- 5 The largest interpolation errors are located in empty grid cells at boundary of the ice sheet along the margins, as data gaps are filled through extrapolation from data inland rather than interpolation between known values. Over higher elevation regions with relatively smooth topography it is more reasonable to assume spatial correlation over interpolation distances of 10 to 50 km, and our chosen interpolation method is more reliable. Within the LRM zone, the median and RMS difference are 6.51 m and 41.70 m, respectively. ~~Because we have not corrected for changes in elevation over time occurring between the acquisition~~  
10 ~~periods of the two datasets within our comparison of interpolated grid cells, there is additional error in elevation differences which is not accounted for in regions where rates of elevation change are large.~~We note that, because the elevation rate is unknown where there is no model solution, we have not corrected for temporal changes in elevation between the acquisition periods of the two datasets within our evaluation of interpolated grid cells. As a result, the reported values represent an upper bound of the elevation difference which includes errors due to both interpolation and elevation change — if present within an  
15 interpolated grid cell.

### 3.3 Comparison of currently available DEMs

- We compare the accuracy of the new CryoSat-2 DEM over the ice shelves, Antarctic Peninsula, West Antarctica and East Antarctica with three other publically available Antarctic DEMs: Bedmap2 (Fretwell et al., 2013), and DEMs generated from ERS-1 and ICESat data (Bamber et al., 2009), and CryoSat-2 data (Helm et al., 2014). To ensure an equivalent comparison  
20 dataset, we only use airborne elevation measurements which reside in an observed grid cell of the presented CryoSat-2 DEM (see Fig. 7). For all four DEMs we use the same evaluation method as described in Sect. 2.4. From the calculated median and root mean squared differences, the new CryoSat-2 DEM we present here is comparable to, or an improvement upon currently available DEMs in all four regions (Fig. 8). In areas of high rates of elevation change, it is worth noting that all four DEMs will exhibit larger biases due to real changes in surface elevation between the acquisition periods of the respective datasets,  
25 and that these differences may be larger in the DEMs containing older ERS-1 and ICESat data (Bedmap2, Bamber et al., 2009). Although another recent DEM of Antarctica (Fei et al., 2017) formed using  $1.7 \times 10^7$  elevation measurements acquired by CryoSat-2 between 2012 and 2014 is not available for direct assessment, it has a reported accuracy of approximately 1 m for the high elevation region at the Domes, 4 m for the ice shelves and over 150 m for mountainous and coastal areas.



## 4 Conclusions

We present a new DEM of Antarctica derived from a spatio-temporal analysis of CryoSat-2 data acquired between July 2010 and July 2016. The DEM is posted at a modal resolution of 1 km and contains an elevation measurement in 94 % and 98 % of ice sheet and ice shelf grid cells, respectively; elevation in a further 5 % of the domain is estimated via ordinary kriging. We evaluate the accuracy of the DEM through comparison to an extensive independent set of airborne laser altimeter elevation measurements, acquired over a contemporaneous time period and in a wide range of locations across the Antarctic ice sheet and ice shelves. From a comparison at grid cells acquired in both data sets, the median and RMS difference between the DEM and airborne data are -0.30 m and 13.50 m, respectively. The largest elevation differences occur in areas of high slope and where CryoSat-2 operates in Low Resolution Mode, where the altimeter ranges to the peaks of undulating terrain and under samples troughs. Using the slope-dependent uncertainties and the wider distribution of slopes, we estimate the overall accuracy of the DEM to be 9.5 m where elevations are formed from satellite data alone. In areas where the DEM is interpolated, the median and RMS differences rise to 19.84 m and 131.13 m, respectively. Through comparisons to an equivalent validation dataset in four individual Antarctic regions, we find the new CryoSat-2 DEM to be comparable to, or an improvement upon, three publically available and widely used Antarctic DEMs.

## 15 Acknowledgements

The new CryoSat-2 DEM ~~is~~will be made freely available to users via the Centre for Polar Observation and Modelling data portal (<http://www.cpom.ucl.ac.uk/csopr/>) and via the European Space Agency (ESA) CryoSat Operational Portal (<https://earth.esa.int/web/guest/missions/esa-operational-eo-missions/cryosat>). This work was led by the NERC Centre for Polar Observation and Modelling, supported by the Natural Environment Research Council (NERC) (cpom300001), with the support of grant (4000107503/13/I-BG). We acknowledge ESA for the provision of CryoSat-2 data (available at <https://earth.esa.int/web/guest/-/cryosat-products>), ESA's Antarctic Ice Sheet\_cci, and the National Snow and Ice Data Center for the provision of IceBridge airborne altimetry data (available at <https://nsidc.org/icebridge/portal>). We also acknowledge the authors of the three digital elevation models used in this study, all of which are freely available online. T.\_S is funded through the NERC iSTAR Programme and NERC grant number NE/J005681/1. A.\_E.\_H is funded from the European Space Agency's support to Science Element program, and an independent research fellowship (4000112797/15/I-SBo). We thank the Editor and three anonymous reviewers for their comments, which helped improve the manuscript.

## References

Armitage, T., Wingham, D., and Ridout, A.: Meteorological origin of the static crossover pattern present in low-resolution-mode CryoSat-2 data over Central Antarctica, IEEE Geosci. Remote S., 11, 1295–1299, doi:10.1109/LGRS.2013.2292821, 2013.

- Bamber, J. L., Gomez-Dans, J. L., and Griggs, J. A.: A new digital elevation model of the Antarctic derived from combined satellite radar and laser data – Part 1: Data and methods, *The Cryosphere*, 3, 101-111, doi:10.5194/tc-3-101-2009, 2009.
- 5 Blankenship, D. D., Young D. D., Kempf, S., Roberts, J. L., van Ommen, T., Forsberg, R., Siegert, M. J., Palmer, S. J., and Dowdeswell, J. A.: IceBridge Riegl Laser Altimeter L2 Geolocated Surface Elevation Triplets, Boulder, Colorado USA, NASA DAAC at the National Snow and Ice Data Center. doi:10.5067/JV9DENETK13E, 2013.
- Cook, A. J., Murray, T., Luckman, A., Vaughan, D. G, and Barrand, N. E.: A new 100-m Digital Elevation model of the  
10 Antarctic Peninsula derived from ASTER Global DEM: methods and accuracy assessment, *Earth Syst. Sci. Data*, 4, 129-142, doi:10.5194/essd-4-129-2012, 2012.
- Cornford, S. L., Martin, D. F., Payne, A. J., Ng, E. G., Le Brocq, A. M., Gladstone, R. M., Edwards, T. L., Shannon, S. R., Agosta, C., van den Broeke, M. R., Hellmer, H. H., Krinner, G., Ligtenberg, S. R. M., Timmermann, R., and Vaughan, D. G.:  
15 Century-scale simulations of the response of the West Antarctic Ice Sheet to a warming climate, *The Cryosphere*, 9, 1579-1600, doi:10.5194/tc-9-1573-2015, 2015.
- Davis, C. H.: A robust threshold retracking algorithm for measuring ice-sheet surface elevation change from satellite radar altimeters, *IEEE T. Geosci. Remote*, 35, 974-979, doi:10.1109/36.602540, 1997.  
20
- Davis, C. H. and Ferguson, A. C.: Elevation change of the Antarctic ice sheet, 1995-2000, from ERS-2 satellite radar altimetry, *IEEE T. Geosci. Remote*, 42, 2437-2445, doi:10.1109/TGRS.2004.836789, 2004.
- DiMarzio, J., Brenner, A., Schutz, R., Shuman, C. A., and Zwally, H. J.: GLAS/ICESat 500m laser altimetry digital elevation  
25 model of Antarctica, Boulder, Colorado, USA. National Snow and Ice Data Center, Digital Media, 2007.
- ESA: CryoSat-2 Product Handbook, ESRIN-ESA and Mullard Space Science Laboratory – University College London, available at: <http://emits.sso.esa.int/emits-doc/ESRIN/7158/CryoSat-PHB-17apr2012.pdf> (last accessed: 02 October 2017), 2012.  
30
- Fei, L., Feng, X., Sheng-Kai, Z., Dong-Chen, E., Xiao, C., Wei-Feng, H., Le-Xian, Y., and Yao-Wen, Z.: DEM Development and precision analysis for Antarctic ice sheet using CryoSat-2 altimetry data, *Chinese J. Geophys.*, 60, 231-243, doi:10.1002/cjg2.30041, 2017.

- Flament, T. and Rémy, F.: Dynamic thinning of Antarctic glaciers from along-track repeat radar altimetry, *J. Glaciol.*, 58, 830-840, doi:10.3189/2012JoG11J118, 2012.
- Fretwell, P., Pritchard, H. D., Vaughan, D. G., Bamber, J. L., Barrand, N. E., Bell, R., Bianchi, C., Bingham, R. G., Blankenship, D. D., Casassa, G., Catania, G., Callens, D., Conway, H., Cook, A. J., Corr, H. F. J., Damaske, D., Damm, V., Ferraccioli, F., Forsberg, R., Fujita, S., Gim, Y., Gogineni, P., Griggs, J. A., Hindmarsh, R. C. A., Holmlund, P., Holt, J. W., Jacobel, R. W., Jenkins, A., Jokat, W., Jordan, T., King, E. C., Kohler, J., Krabill, W., Riger-Kusk, M., Langley, K. A., Leitchenkov, G., Leuschen, C., Luyendyk, B. P., Matsuoka, K., Mouginot, J., Nitsche, F. O., Nogi, Y., Nost, O. A., Popov, S. V., Rignot, E., Ripplin, D. M., Rivera, A., Roberts, J., Ross, N., Siegert, M. J., Smith, A. M., Steinhage, D., Studinger, M., Sun, B., Tinto, B. K., Welch, B. C., Wilson, D., Young, D. A., Xiangbin, C., and Zirizzotti, A.: Bedmap2: improved ice bed, surface and thickness datasets for Antarctica, *The Cryosphere*, 7, 375–393, doi:10.5194/tc-7-375-2013, 2013.
- Griggs, J. A. and Bamber, J. L.: A new 1 km digital elevation model of Antarctica derived from combined radar and laser data – Part 2: Validation and error estimates, *The Cryosphere*, 3, 113-123, doi:10.5194/tc-3-113-2009, 2009.
- Helm, V., Humbert, A., and Miller, H.: Elevation and elevation change of Greenland and Antarctica derived from CryoSat-2, *The Cryosphere*, 8, 1539-1559, doi:10.5194/tc-8-1539-2014, 2014.
- Isaaks, E. H. and Srivastava, R. M.: *An Introduction to Applied Geostatistics*, Oxford University Press, New York, 1989.
- Koenig, L., Martin, S., Studinger, M., and Sonntag, J.: Polar Airborne Observations Fill Gap in Satellite Data, *EOS Trans.*, 91, 333-334, doi:10.1029/2010EO380002, 2010.
- Khvorostovsky, K.S.: Merging and analysis of elevation time series over Greenland ice sheet from satellite radar altimetry, *IEEE T. Geosci. Remote*, 50, 23-36, doi:10.1109/TGRS.2011.2160071, 2012.
- Kitanitis, P. K.: *Introduction to Geostatistics: Applications in Hydrogeology*, Cambridge University Press, Cambridge, 1997.
- Korona J., Berthier, E., Bernard, M., Rémy, F., and Thouvenot, E.: SPIRIT. SPOT 5 stereoscopic survey of Polar Ice: Reference Images and Topographies during the fourth International Polar Year (2007-2009), *ISPRS J. Photogramm.*, 64, 204-212, doi:10.1016/j.isprsjprs.2008.10.005, 2009.
- Krabill, W. B.: *IceBridge ATM L2 Icessn Elevation, Slope, and Roughness Version 2*, Boulder, Colorado USA, NASA DAAC at the National Snow and Ice Data Center, Digital Media, doi:10.5067/CPRXXK3F39RV, 2016.

- Krabill, W. B., Hanna, E., Huybrechts, P., Abdalati, W., Cappelen, J., Csatho, B., Frederick, E., Manizade, S., Martin, C., Sonntag, J., Swift, R., Thomas R., and Yungel, J.: Greenland Ice Sheet: Increased Coastal Thinning, *Geophys. Res. Lett.*, 31, L24402, doi:10.1029/2004GL021533, 2004.
- 5
- Kwok, R., Cunningham, G. F., Manizade, S. S., and Krabill W. B.: Arctic sea ice freeboard from IceBridge acquisitions in 2009: Estimates and comparisons with ICESat, *J. Geophys. Res.*, 117, C02018, doi:10.1029/2011JC007654, 2012.
- Levinsen, J. F., Howat, I. M., Tscherning, C. C.: Improving maps of ice-sheet surface elevation change using combined laser altimeter and stereoscopic elevation model data, *J. Glaciol.*, 59, 524-532, doi:10.3189/2013JoG12J114, 2013.
- 10
- Liu, H., Jezek, K. C., Li, B., and Zhao, Z.: Radarsat Antarctic Mapping Project Digital Elevation Model Version 2 Boulder, Colorado, USA. National Snow and Ice Data Center, Digital Media, 2001.
- Liu, H., Jezek, K. C., Li, B., and Zhao, Z.: Radarsat Antarctic Mapping Project Digital Elevation Model Version 2 Boulder, Colorado, USA. National Snow and Ice Data Center, Digital Media, 2001.
- 15
- McMillan, M., Shepherd, A., Sundal, A., Briggs, K., Muir, A., Ridout, A., Hogg, A., and Wingham, D.: Increased ice losses from Antarctica detected by CryoSat-2, *Geophys. Res. Lett.*, 41, 3899–3905, doi:10.1002/2014GL060111, 2014GL060111, 2014.
- Mouginot, J., Scheuchl, B., and Rignot, E.: Mapping of Ice Motion in Antarctica Using Synthetic-Aperture Radar Data, *Remote Sens.*, 4, 2753-2767, doi:10.3390/rs4092753, 2012.
- 20
- Rignot, E., Mouginot, J., and Scheuchl, B.: Ice Flow of the Antarctic Ice Sheet, *Science*, 333, 1427-1430, doi:10.1126/science.1208336, 2011a.
- Rignot, E., Velicogna, I., van den Broeke, M. R., Monaghan, A., and Lenaerts, J. T. M.: Acceleration of the contribution of the Greenland and Antarctic ice sheets to sea level rise, *Geophys. Res. Lett.*, 38, L05503, doi:10.1029/2011GL046583, 2011b.
- Ritz, C., Edwards T. L., Durand, G., Payne, A. J., Peyaud, V., and Hindmarsh. R. C. A.: Potential sea-level rise from Antarctic ice-sheet instability constrained by observations, *Nature*, 528, 115-118, doi:10.1038/nature16147, 2015.
- 30
- Shepherd, A., Ivins, E. R., Geruo, A., Barletta, V. R., Bentley, M. J., Bettadpur, S., Briggs, K. H., Bromwich, D. H., Forsberg, R., Galin, N., Horwath, M., Jacobs, S., Joughin, I., King, M. A., Lenaerts, J. T. M., Li, J., Ligtenberg, S. R. M., Luckman, A., Luthcke, S. B., McMillan, M., Meister, R., Milne, G., Mouginot, J., Muir, A., Nicolas, J. P., Paden, J., Payne, A. J., Pritchard, H., Rignot, E., Rott, H., Sorensen, L. S., Scambos, T. A., Scheuchl, B., Schrama, E. J. O., Smith, B., Sundal, A. V., van

- Angelen, J. H., van de Berg, W. J., van den Broeke, M. R., Vaughan, D. G., Velicogna, I., Wahr, J., Whitehouse, P. L., Wingham, D. J., Yi, D., Young, D., and Zwally, H. J.: A reconciled estimate of ice-sheet mass balance, *Science*, 338, 1183–1189, doi:10.1126/science.1228102, 2012.
- 5 Sutterly, T. C., Velicogna, I., Rignot, E., Mouginot, J., Flament, T., van den Broeke, M. R., van Wessem, J., M., and Reijmer, C. H.: Mass loss of the Amundsen Sea Embayment of West Antarctica from four independent techniques, *Geophys. Res. Lett.*, 41, 8421-8428, doi:10.1002/2014GL061940, 2014.
- Wingham, D. J. and Wallis, D. W.: The Rough Surface Impulse Response of a Pulse-Limited Altimeter With an Elliptical  
10 Antenna Pattern, *IEEE Antenn. Wirel. PR.*, 9, 232-235, doi:10.1109/LAWP.2010.2046471, 2010.
- Wingham, D. J., Rapley, C. G., and Griffiths, H.: New techniques in satellite altimeter tracking systems, in: *Proceedings of the IGARSS Symposium*, vol. SP-254, 1339–1344, edited by: Guyenne, T. D. and Hunt, J. J., European Space Agency, Zurich, September 1986, 1986.
- 15 Wingham, D. J., Phalippou, L., Mavrocordatos, C., and Wallis, D.: The Mean Echo Cross Product From a Beamforming Interferometric Altimeter and Their Application to Elevation Measurement, *IEEE T. Geosci. Remote*, 42, 2305-2323, doi:10.1109/TGRS.2004.834352, 2004.
- 20 Wingham, D., Francis, C. R., Baker, S., Bouzinac, C., Cullen, R., de Chateau-Thierry, P., Laxon, S. W., Mallow, U., Mavrocordatos, C., Phalippou, L., Ratier, G., Rey, L., Rostan, F., Viau, P., and Wallis, D.: CryoSat: a mission to determine the fluctuations in Earth’s land and marine ice fields, *Adv. Space Res.*, 37, 841–871, doi:10.1016/j.asr.2005.07.027, 2006.
- 25 Young, D. A., Kempf, S. D., Blankenship, D. D., Holt, and Morse, D. L.: New airborne laser altimetry over the Thwaites catchment, West Antarctica, *Geochem. Geophys. Geosy.*, 9, Q06006, doi:10.1029/2007GC001935, 2008.
- Zwally, H. J., Giovinetto, M. B., Beckley, M. A., and Saba, J. J. L.: Antarctic and Greenland Drainage Systems, available at: [http://icesat4.gsfc.nasa.gov/cryo\\_data/ant\\_grn\\_drainage\\_systems.php](http://icesat4.gsfc.nasa.gov/cryo_data/ant_grn_drainage_systems.php) (last accessed: 15 May 2017), 2012.

Year	Number of compared grid cells	Median difference (m)	RMS difference (m)
2009	3490	-4.97	11.35
2011	2819	-2.08	8.56
2014	2794	0.05	3.97

**Table 1: Statistics of the comparison between observed DEM grid cells derived from 1 km model fits, and ATM elevation measurements in the Pine Island Glacier drainage basin. The airborne data are separated into the year of acquisition to demonstrate the effect of ice dynamical thinning in this region on the elevation difference. The effective date of the DEM is July 2013.**

Region	Observed			Interpolated		
	Number of compared grid cells	Median difference (m)	RMS difference (m)	Number of compared grid cells	Median difference (m)	RMS difference (m)
Ice sheet	230165	-0.27	13.36	32933	25.37	138.62
Ice shelves	40081	-0.42	14.31	4772	1.20	30.96
<u>Antarctic</u> Peninsula	6820	-1.12	22.40	7473	82.21	191.07
West Antarctica	60452	-0.86	11.43	8783	11.78	96.15
East Antarctica	162893	-0.17	13.60	14679	19.62	117.77
LRM	73867	0.26	7.15	1683	6.51	41.70
SARIn (ice sheet only)	156298	-0.82	15.45	31250	28.65	141.97
Total	270246	-0.30	13.50	37655	19.84	131.13

**Table 2: Statistics of the comparison between observed and interpolated DEM grid cells and airborne elevation measurements for individual Antarctic regions and mode mask areas. In total, only 5% and 2% of DEM elevation values are obtained through interpolation for the ice sheet and ice shelves, respectively.**

Slope (°)	LRM		SARIn	
	RMS difference (m)	LRM area coverage (km <sup>2</sup> )	RMS difference (m)	SARIn area coverage (km <sup>2</sup> )
0-0.25	4.90	5481579	6.37	1373258
0.25-0.5	11.24	975624	8.54	1338826
0.5-0.75	19.85	143420	13.50	775083
>0.75	29.59	93660	24.26	1551836

**Table 3: RMS differences between observed DEM grid cells airborne elevation measurements for four slope bands, separated into the LRM and SARIn mode mask areas for the Antarctic ice sheet. The area of each region represented by the four slope bands is also provided.**



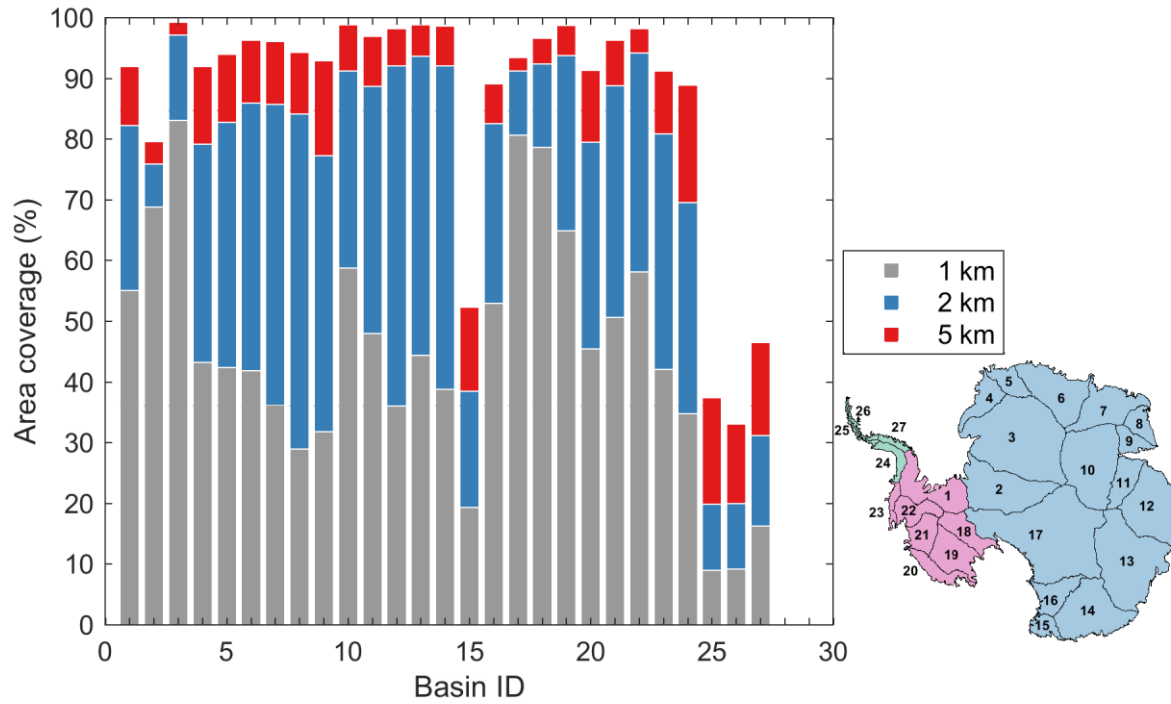


Figure 1: Area coverage of elevation values provided by the model fit solution (Eq. (1)) of CryoSat-2 measurements for the Antarctic ice sheet, with a grid cell sizing of 1 km<sup>2</sup>, 2 km<sup>2</sup> and 5 km<sup>2</sup>. Solid black lines and numbers (inset) show the boundaries and ID numbers of the 27 drainage basins used (Zwally et al., 2012). East Antarctica and the Antarctic Peninsula are defined as numbers 2 to 17 and 24 to 27, respectively, and the remaining numbers define West Antarctica.

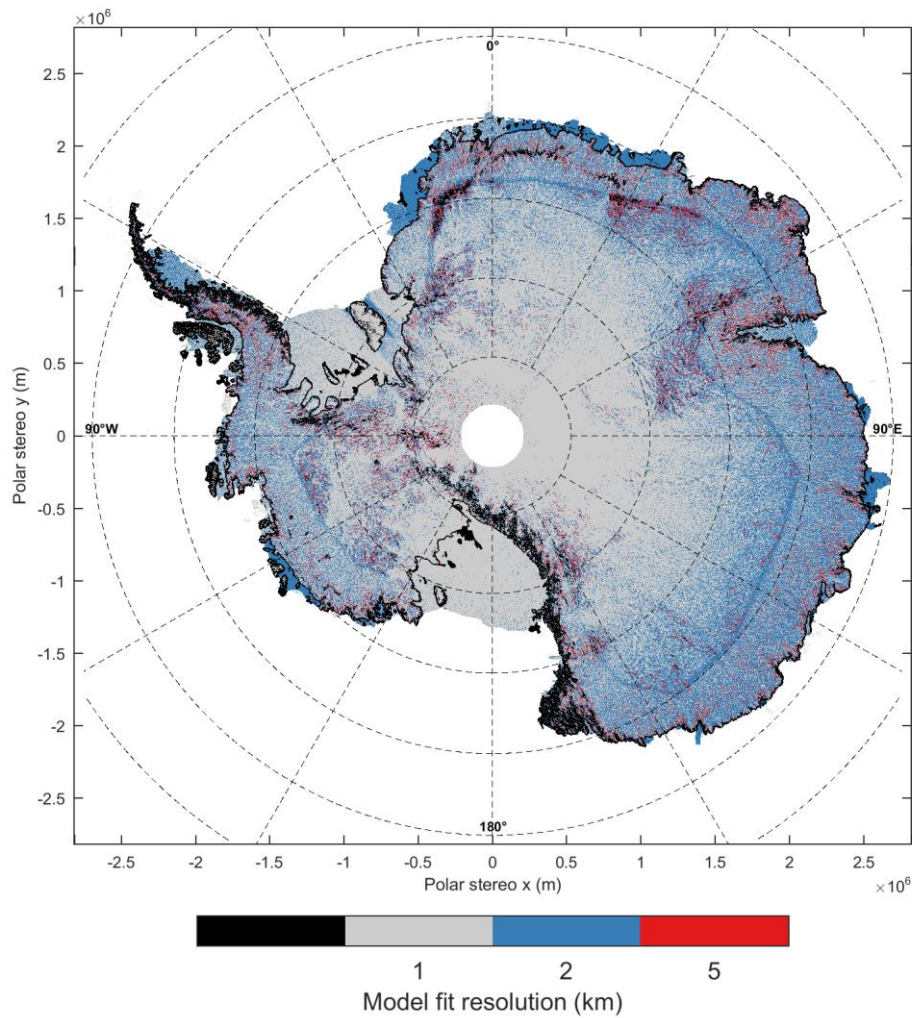
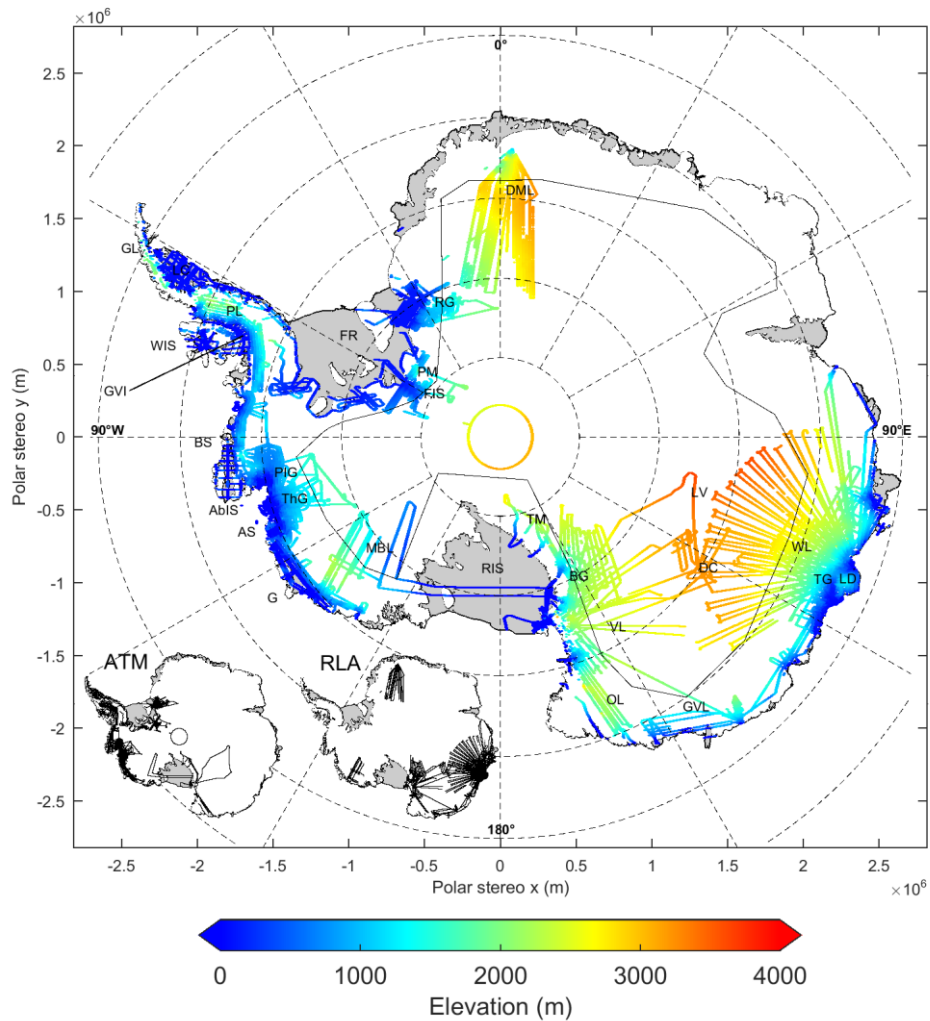
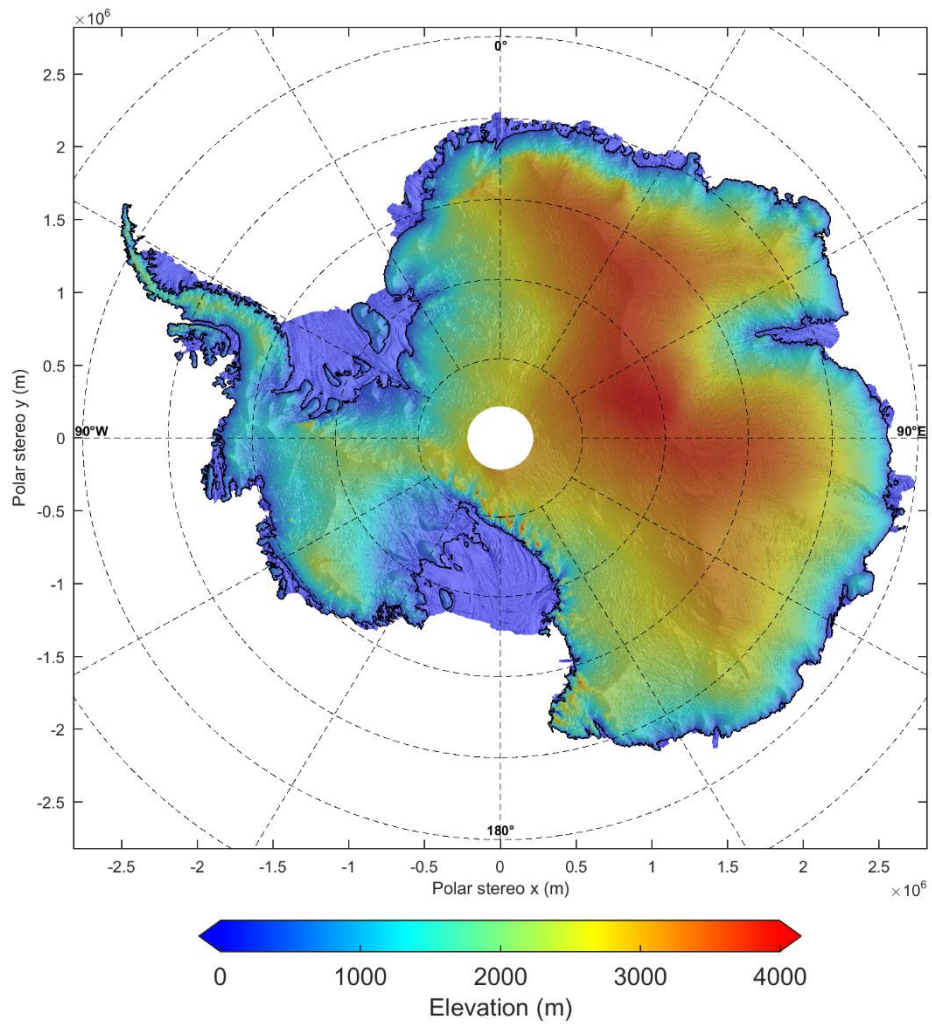


Figure 2: The grid cell resolution of the model fit method used to derive the surface elevation in each 1 km grid cell. Elevation values obtained from the 2 km and 5 km model fits are oversampled to the modal DEM resolution of 1 km. A black grid cell denotes a cell that contains an interpolated value. For the grounded ice sheet, approximately 60%, 30% and 5% of elevation values are derived from 1, 2 and 5 km model fits, respectively. For the ice shelves, 75% of elevations are calculated with 1 km model fits, and 23% from 2 km model fits. The remaining 5% of ice sheet and 2% of ice shelf values are interpolated using ordinary kriging. At the mode mask boundary, where CrvoSat-2 switches between LRM and SARIn operating modes, grid cells are predominantly derived from 2 km model fits, as there are a reduced number of elevation measurements available to constrain model fits at a resolution of 1 km.



**Figure 3: IceBridge airborne dataset used to evaluate the DEM, acquired between December 2008 and December 2014. The mode mask boundary (solid black line) between CryoSat-2 LRM and SARIn modes is also shown. (inset) Locations of the individual ATM and RLA airborne datasets. Labelled are the following locations of interest: AbIS: Abbot Ice Shelf, AS: Amundsen Sea, BS: Bellingshausen Sea, BG: Byrd Glacier, DC: Dome C, DML: Dronning Maud Land, FIS: Foundation Ice Stream, FR: Filchner-Ronne Ice Shelf, G: Getz, GL: Graham Land, GVI: George VI Ice Shelf, GVL: George V Land, LC: Larsen-C Ice Shelf, LD: Law Dome, LV: Lake Vostok, MBL: Marie Byrd Land, OL: Oates Land, PIG: Pine Island Glacier, PL: Palmer Land, PM: Pensacola Mountains, RG: Recovery Glacier, RIS: Ross Ice Shelf, TG: Totten Glacier, ThG: Thwaites Glacier, TM: Transantarctic Mountains, VL: Victoria Land, WIS: Wilkins Ice Shelf, WL: Wilkes Land.**



**Figure 4: A new elevation model of Antarctica derived from 6 years of CryoSat-2 radar altimetry data acquired between July 2010 and July 2016.**

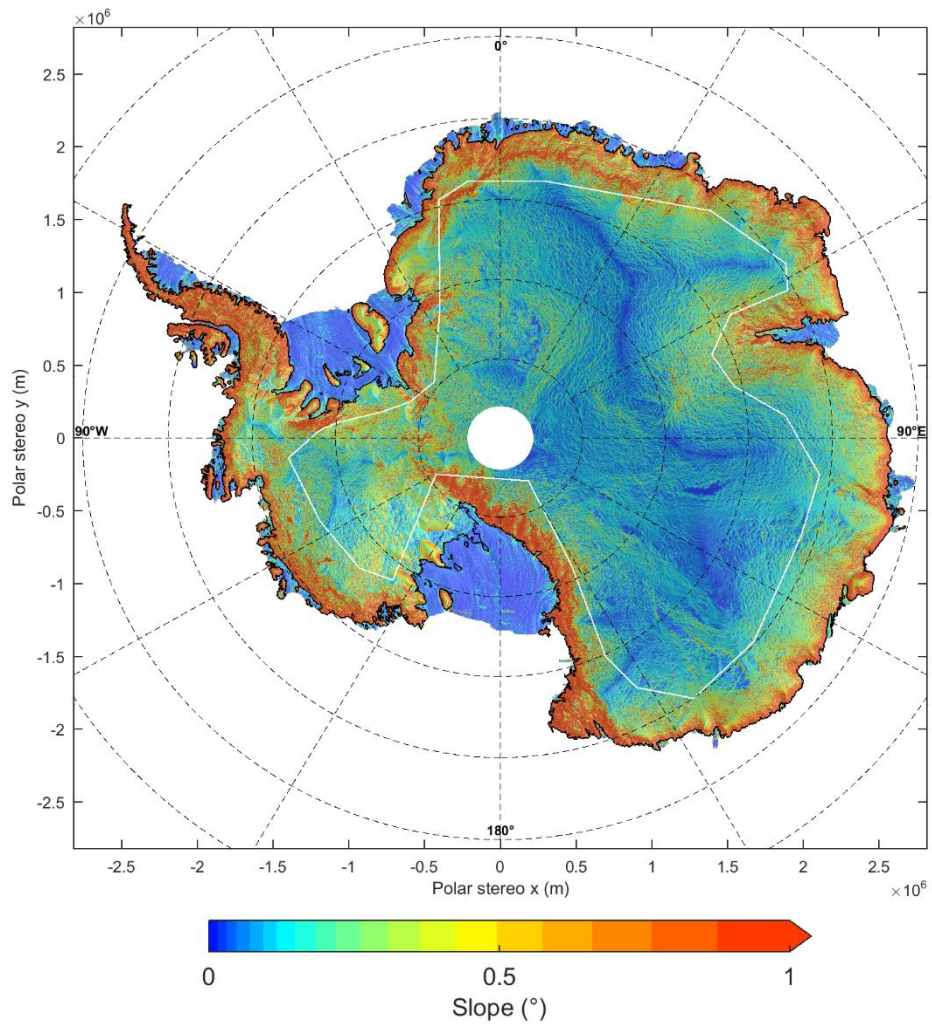
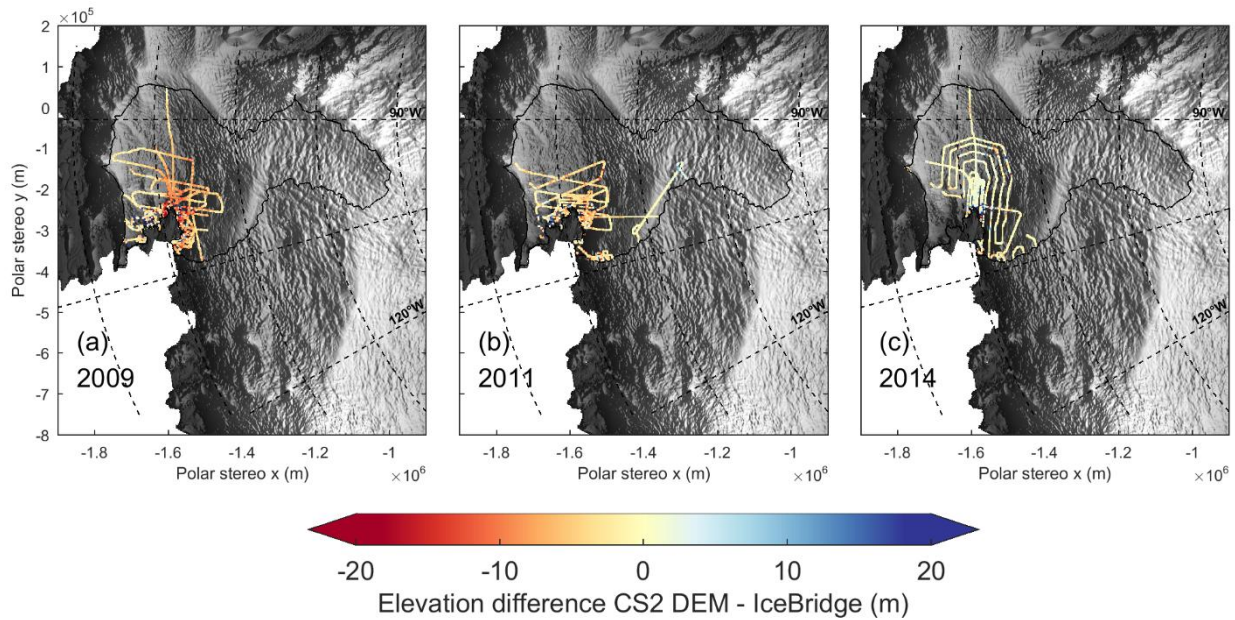
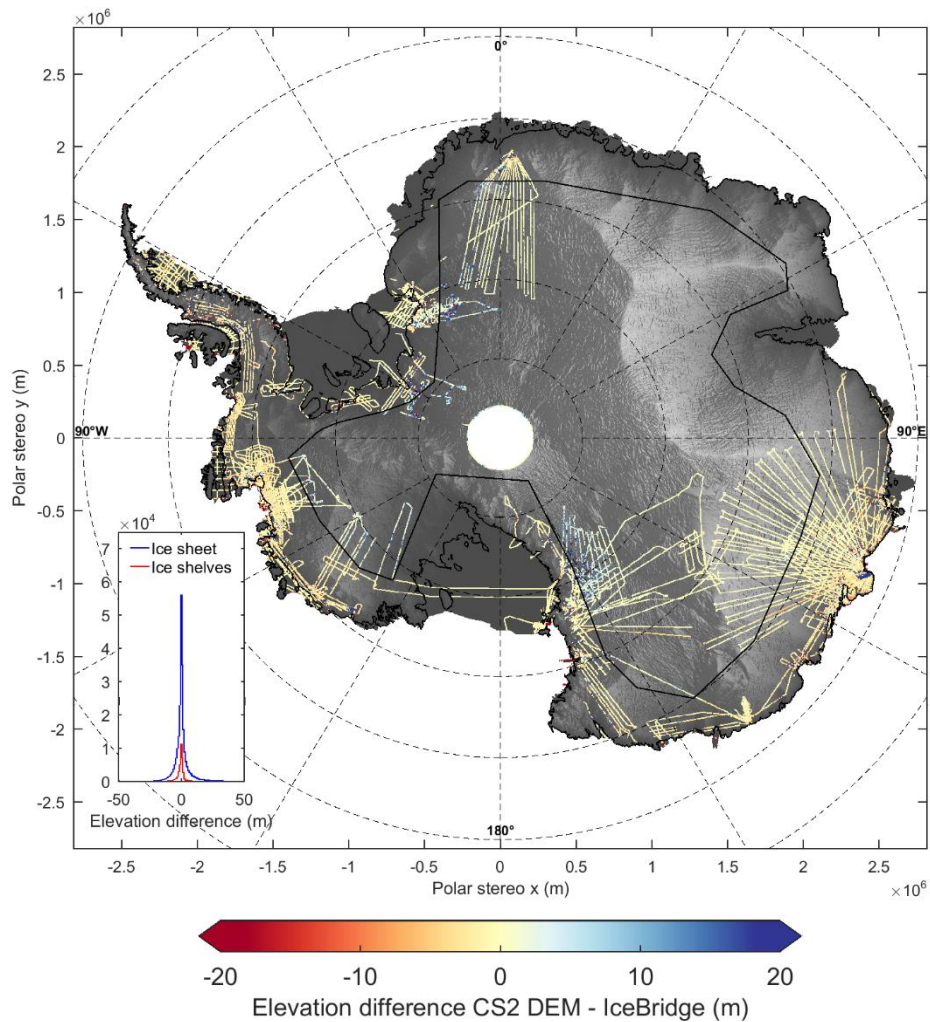


Figure 5: Surface slopes of Antarctica posted at a resolution of 1 km, derived from the digital elevation model. The mode mask boundary between CryoSat-2 LRM and SARIn modes is also shown in white.



**Figure 6: Difference between observed DEM grid cells derived from 1 km model fits and IceBridge ATM elevation measurements for the Pine Island Glacier region in West Antarctica for ATM flight surveys undertaken in the years (a) 2009, (b) 2011 and (c) 2014. The DEM has an effective time stamp of July 2013. The boundary of the Pine Island Glacier drainage basin (whitesolid black line) is also shown (Zwally et al., 2012).**



**Figure 7: Difference between CryoSat-2 DEM elevation and airborne laser altimeter measurements in observed grid cells. The mode mask boundary between CryoSat-2 LRM and SARIn modes is also shown as a solid black line. Elevation differences are overlaid on a shaded relief plot of the DEM. (inset) Distribution of the elevation differences (DEM – airborne) for the ice sheet and ice shelves.**

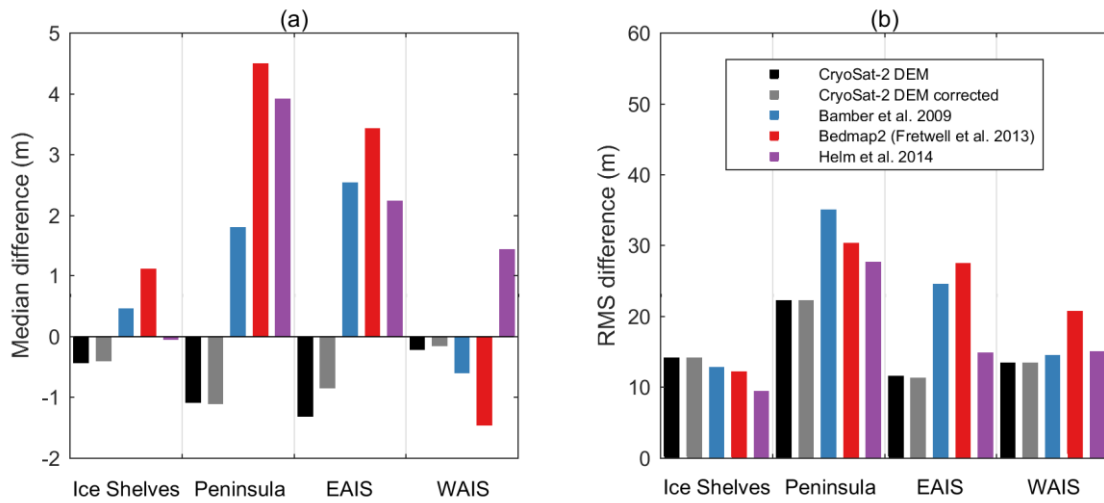


**Figure 8: (a) Median and (b) RMS differences between airborne elevation measurements calculated over the ice shelves, Antarctic Peninsula, West Antarctica (WAIS) and East Antarctica (EAIS) for the new CryoSat-2 DEM presented in this report, and three publicly available Antarctic DEMs. CryoSat-2 DEM comparisons with the elevation change correction applied (Table 2) are plotted as square outlines grey bars.**



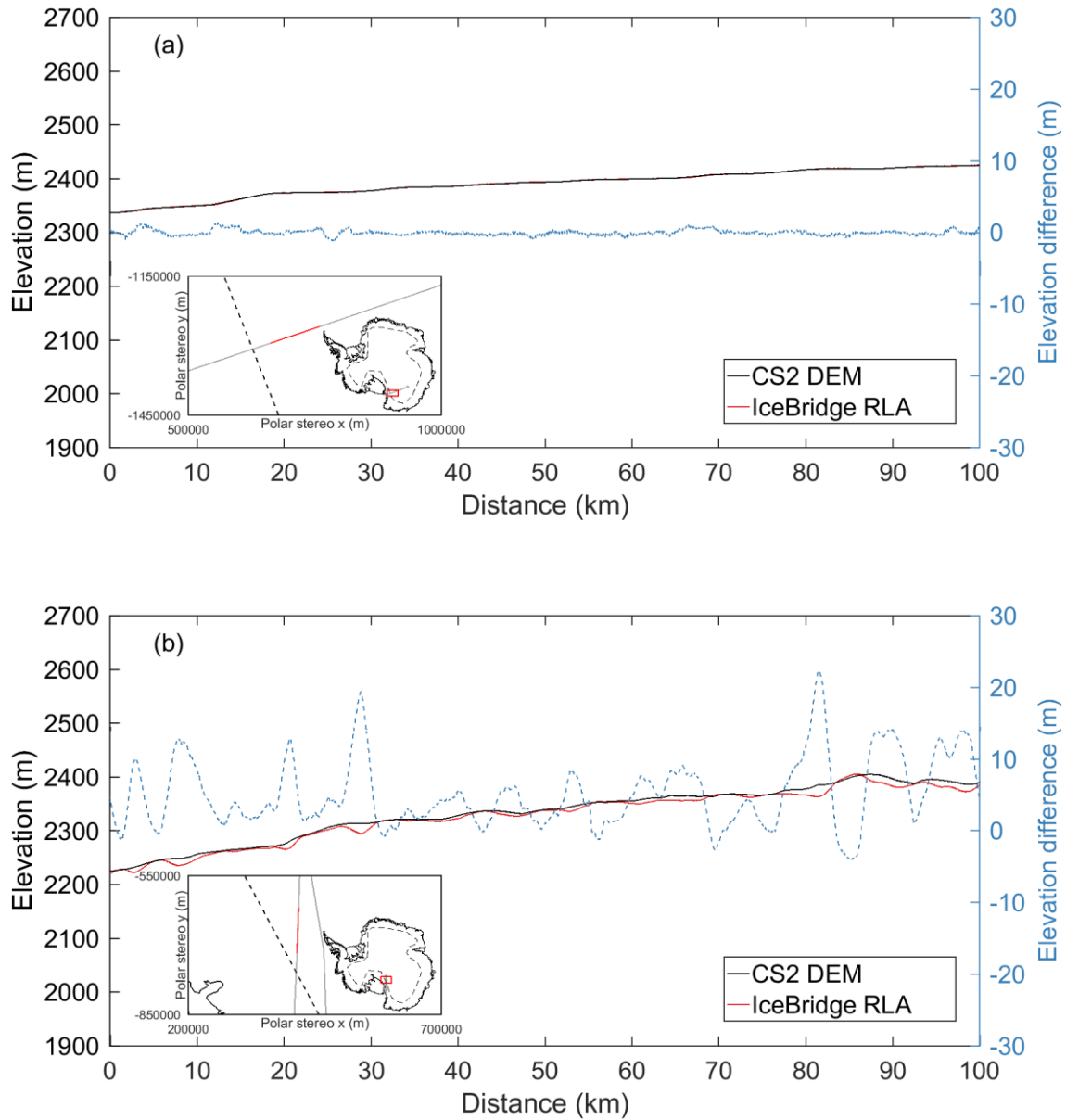


**Figure 9: CryoSat-2 LRM, and IceBridge RLA elevation profiles for 100 km flight path sections obtained in (a) Victoria Land, where surface slopes are low, and (b) inland from Byrd Glacier, where surface slopes are high. Elevation differences (CS2 DEM – airborne) are plotted in blue to the right hand scale. (Inset) locations of RLA flight paths, with the profile section highlighted in red. The LRM/SARIn/ARM mode mask boundary is shown as a dashed line.**

# Supplementary material for: A new Digital Elevation Model of Antarctica derived from CryoSat-2 altimetry

Thomas Slater<sup>1</sup>, Andrew Shepherd<sup>1</sup>, Malcolm McMillan<sup>1</sup>, Alan Muir<sup>2</sup>, Lin Gilbert<sup>2</sup>, Anna E. Hogg<sup>1</sup>, Hannes Konrad<sup>1</sup>, Tommaso Parrinello<sup>3</sup>

<sup>1</sup>Centre for Polar Observation and Modelling, School of Earth and Environment, University of Leeds, Leeds, LS2 9JT, United Kingdom

<sup>2</sup>Centre for Polar Observation and Modelling, University College London, London, WC1E 6BT, United Kingdom

<sup>3</sup>ESA ESRIN, Via Galileo Galilei, 00044 Frascati RM, Italy

*Correspondence to:* Thomas Slater ([py10ts@leeds.ac.uk](mailto:py10ts@leeds.ac.uk))

## 1 Elevation retrieval from CryoSat-2: data filtering approach

After the application of Eq. (1) to our selected CryoSat-2 dataset, we apply a series of quality filters to remove unrealistic elevation estimates from poorly constrained model fits. In order to identify these unrealistic elevation estimates, we introduce constraints based upon (i) data availability, (ii) data quality and (iii) physical plausibility (Table S1). Controls on data availability include a minimum number of data points, and length of the elevation time series within each grid cell. In each case, threshold values have been tested and found to be optimal. A minimum of 15 data points, and time series length of at least 2 years ensures that each model fit is constrained by sufficient data. We remove poorly constrained fits by introducing thresholds on the goodness of fit, with maximum values of the root mean squared difference of the elevation residuals from the model fit, and 1-sigma uncertainty in the elevation rate being 10 m and 0.4 m yr<sup>-1</sup>, respectively. Finally, we remove any estimates that are not physically plausible. Maximum rates of elevation change have been reported to be 9 m yr<sup>-1</sup> in Antarctica (McMillan et al., 2014), so we remove any elevation rate estimate with a magnitude exceeding 10 m yr<sup>-1</sup>. In addition, we impose a maximum quadratic surface slope value of 5 ° to maintain physically plausible glacier driving stresses — averaged over the grid cell resolution — which are controlled by the slope.

After data filtering, the model fit provides an elevation estimate for 60 %, 91 % and 94 % of grid cells within the Antarctic ice sheet at resolutions of 1 km, 2 km and 5 km, respectively. For the Antarctic ice shelves, 75 % and 98 % of grid cells at resolutions of 1 km and 2 km, respectively, contain an elevation estimate from our model fit approach after quality filtering has been applied.

Parameter	Selection criteria
Number of data points	$\leq 15$
Time series length (yrs)	$\leq 2$
Root mean squared difference of elevation residuals from model fit (m)	$\geq 10$
1-sigma uncertainty in dh/dt ( $\text{m yr}^{-1}$ )	$\geq 0.4$
$ \text{dh}/\text{dt} $ ( $\text{m yr}^{-1}$ )	$\geq 10$
Surface slope ( $^{\circ}$ )	$\geq 5$

**Table S1: Selection criteria used to remove elevation estimates resulting from poorly constrained model fits.**

## 2 Uncertainty map

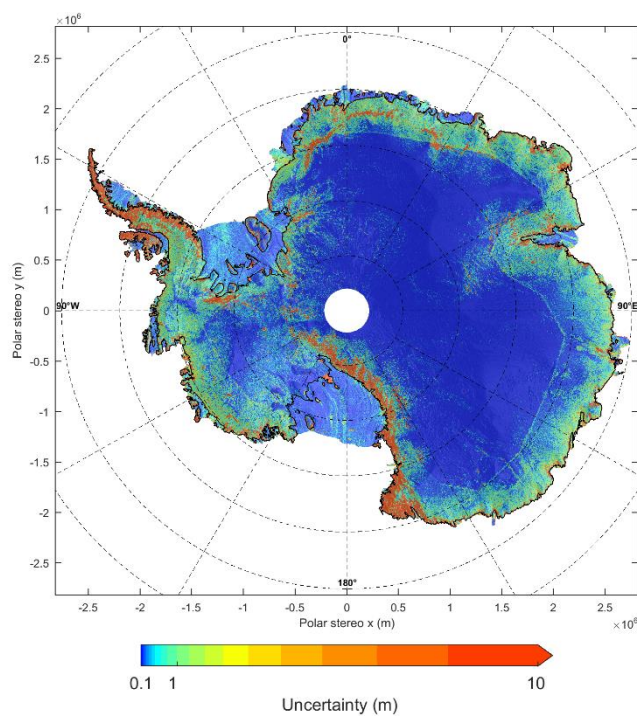


**Figure S1: Uncertainty map of the new CryoSat-2 Antarctic DEM, calculated from the root mean squared difference of elevation residuals in observed grid cells, and the kriging variance error in interpolated grid cells.**

## References

McMillan, M., Shepherd, A., Sundal, A., Briggs, K., Muir, A., Ridout, A., Hogg, A., and Wingham, D.: Increased ice losses from Antarctica detected by CryoSat-2, *Geophys. Res. Lett.*, 41, 3899–3905, doi:10.1002/2014GL060111, 2014GL060111, 2014.